chemengineering

MDPI

Specifically Designed Ionic Liquids—Formulations, Physicochemical Properties, and Electrochemical Double Layer Storage Behavior

Zheng Yue [1], Qiang Ma [2], Xinyi Mei [3], Abigail Schulz [1], Hamza Dunya [1], Dana Alramahi [1], Christopher McGarry [2], Jim Tufts [1], Amartya Chakrabarti [4], Rituparna Saha [1] and Braja K. Mandal [1,*]

[1] Department of Chemistry, Illinois Institute of Technology, Chicago, IL 60616, USA; zyue1@hawk.iit.edu (Z.Y.); aschulz2@hawk.iit.edu (A.S.); hdunya@hawk.iit.edu (H.D.); dalramah@hawk.iit.edu (D.A.); jim.tufts@gmail.com (J.T.); saharit@gmail.com (R.S.)
[2] 5X Energy Solutions, Inc., 805 Plainfield Rd., Suite 112, Darien, IL 60561, USA; qma4@hawk.iit.edu (Q.M.); mcgarry@uwalumni.com (C.M.)
[3] National Academy of Economic Security, Beijing Jiaotong University, Beijing 100000, China; xmei3@hawk.iit.edu
[4] Department of Physical Sciences, Dominican University, River Forest, IL 60305, USA; chakama1@hawk.iit.edu
* Correspondence: mandal@iit.edu; Tel.: +1-312-5673446

check for updates

Abstract: Two key features—non-volatility and non-flammability—make ionic liquids (ILs) very attractive for use as electrolyte solvents in advanced energy storage systems, such as supercapacitors and Li-ion batteries. Since most ILs possess high viscosity and are less prone to dissolving common electrolytic salts when compared to traditional electrolytic solvents, they must be formulated with low viscosity thinner solvents to achieve desired ionic conductivity and dissolution of electrolyte salts in excess of 0.5 M concentration. In the past few years, our research group has synthesized several specifically designed ILs (mono-cationic, di-cationic, and zwitterionic) with bis(trifluoromethylsulfonyl)imide (TFSI) and dicyanamide (DCA) as counter anions. This article describes several electrolyte formulations to achieve superior electrolytic properties. The performance of a few representative IL-based electrolytes in supercapacitor coin cells is presented.

Keywords: ionic liquids; di-cationic ionic liquids; zwitterionic liquids; ionic conductivity; viscosity; nonflammable electrolytes; supercapacitor cells

1. Introduction

Lithium-ion batteries (LIBs) are now exclusively used to power hybrid and electric vehicles, due to their high energy density and operational voltage [1–4]. However, current state-of-the-art LIB systems have critical challenges regarding safety, due to the use of highly volatile and extremely flammable organic carbonates, such as ethylene carbonate (EC), dimethyl carbonate (DMC), and diethyl carbonate (DEC) [5–7]. Consequently, in recent years many strategies have been explored to develop alternative electrolytes that have nonflammable characteristics. Solid polymer electrolytes (SPEs) have been studied, but their poor ionic conductivity is the main obstacle [8–10]. Gel polymer electrolytes (GPEs) have been obtained by infusing organic liquid electrolytes into a polymer matrix. Though GPEs display good ionic conductivity, safety concerns caused by volatile and flammable organic solvents cannot be ignored [11,12].

Among the nonflammable or safer electrolytes investigated thus far, ionic liquids (ILs) have been considered as the most promising candidates. In contrast to carbonate-based electrolytes, ILs possess nonflammability, negligible volatility, and high thermal and electrochemical stabilities [13–17]. However, they possess high viscosity, and with a few exceptions, exhibit low pristine ionic conductivity, which deteriorates to an unacceptable value (<1 mS cm^{-1}) when a lithium salt in >0.5 M concentration is added. The viscosity of ILs is known to depend on the molecular frictional forces that are governed by their size. It is known that bulky molecules experience higher friction along with slow diffusion, leading to higher viscosity [18].

How fast a Li-ion cell can be charged or discharged depends on how fast Li$^+$ can be moved from one electrode to the other. During the charge of the graphitic carbon anode, the Li$^+$ charge transfer process of Li$^+$ in the electrolyte to Li in the Li$_x$C$_6$ electrode includes the following three steps:

STEP-1:　Li^+　$\xrightarrow{\text{De-solvation}}$　Li^+　*(before entering Solid Electrolyte Interphase)*

STEP-2:　Li^+　*diffusion through Solid Electrolyte Interphase*　　　　　Li^+　*(denotes a solvated Li$^+$)*

STEP-3:　xLi^+　$+$　C_6　$+$　xe^-　$\xrightarrow{\text{Insertion / Electron-transfer}}$　Li_xC_6
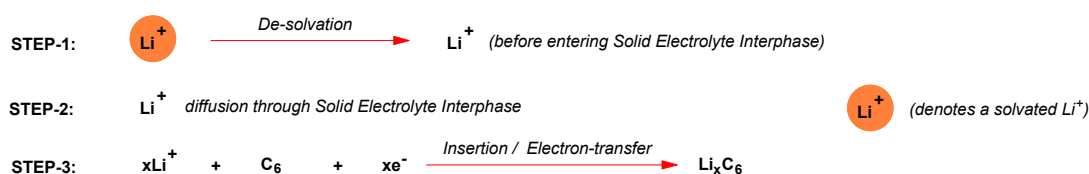
Similar steps would happen at the cathode during discharge. During charging of the cathode, such as lithium nickel cobalt aluminum mixed oxide (LiNi$_y$Co$_z$Al$_{1-y-z}$O$_2$), the charge transfer process includes the following steps [19]:

STEP-4:　$LiNi_yCo_zAl_{1-y-z}O_2$　$\xrightarrow{\text{De-insertion / Electron-transfer}}$　$Li_{1-x}Ni_yCo_zAl_{1-y-z}O_2$　$+$　xLi^+　$+$　xe^-

STEP-5:　Li^+　*diffusion through Cathode Electrolyte Interphase*

STEP-6:　Li^+　$\xrightarrow{\text{Solvation}}$　Li^+
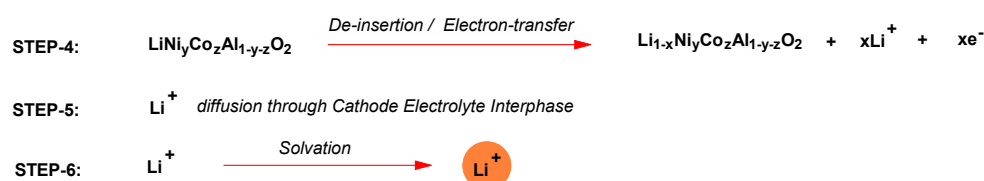
If the conductivity of the electrolyte is poor, then the activation energy of the ion conduction will be very high, which may make steps 1 and 6 rate limiting. Therefore, a high ionic conductivity (>7 mS cm^{-1}) is a must for achieving fast charge/discharge operations (>20C, i.e., three minutes each to complete charge and discharge).

This research work directly addresses the issue of low ionic conductivity of ILs by synthesizing several new specifically designed ILs, fluorine-containing ionic liquids (FILs), dicationic ionic liquids (DILs), and zwitterionic liquids (ZILs). We have also synthesized some previously reported ILs that are not commercially available in order to draw meaningful conclusions. Finally, we have prepared several nonflammable electrolyte formulations for applications in advanced LIBs. We have demonstrated that high energy density supercapacitor cells can be constructed using IL-based electrolytes.

IL-based electrolytes also have applications in electrical double layer capacitors (EDLCs) [20]. Their high electrochemical stability greatly increases the maximum operation voltage (OPV) of the cells [21], which lead to higher energy density. A variety of electrolytes have been developed, including neat ILs [22,23], IL solutions in organic solvents [23,24] and IL-doped polymer solid-state electrolytes [25]. Along with monovalent cationic ILs, DILs and polyvalent cationic ILs have also been considered for EDLC electrolytes [26]. ILs are not only very useful to electrical energy storage devices, but also found valuable in various scientific research and industry areas [27], including enhanced solvents for organic reactions, superior solvents to produce innovative materials, etc. [28,29].

2. Materials and Methods

Most ILs cited in this paper marked "new compounds" have been synthesized by our research group. Some of them have been recently published and properly referenced. In this section, we describe the synthesis of the ILs, which have not published elsewhere.

2.1. Materials

The chloride form of the anion-exchange resin, Amberlite IRA402 Cl, was purchased from Alfa Aesar. Before use, the resin was washed with anhydrous methanol and dried at 40 °C for 48 h to remove the water content. 4 Å molecular sieves (Sigma Aldrich, St. Louis, MO, USA) were activated at 150 °C under high vacuum for 12 h before use. All other reagents and solvents were used without further purification: Chloromethyl methyl ether (Technical grade, Sigma Aldrich); *N*-methyl pyrrolidine (98%) (Alfa Aesar); 1-methyl imidazole (99%) (Alfa Aesar, Haverhill, MA, USA); p-toluenesulfonyl chloride (Sigma Aldrich); propargyl alcohol (99%) (Alfa Aesar); bromoethane (98%) (Sigma Aldrich); 1-chlorobutane (Sigma Aldrich); LiTFSI (99.5%) (SynQuest, Alachua, FL, USA); $NaPF_6$ (99%) (Sigma Aldrich); $NaBF_4$ (97%) (Alfa Aesar); $NaN(CN)_2$ (96%) (Alfa Aesar); diethyl sulfide (98%) (Sigma Aldrich). Other sulfide precursors were prepared and purified by vacuum distillation in our lab [30]. *N*-methyldiethanolamine (NMDE), 2-[2-(dimethylamino) ethoxy] ethanol (DAEE), 2-*tert*-butylamino ethanol (TBAE), triethanol amine (TEA), tetramethylammonium hydroxide (25 wt% in H_2O solution) (TMAH), acrylonitrile, 1,3-propane sultone were purchased from Sigma-Aldrich Company and used as received without further purification. 2-nitropropane (2-NP), from Sigma-Aldrich Company, was freshly distilled before use.

2.2. General Synthetic Procedure of New ILs

Typically, the synthesis of all ILs discussed in this paper was composed of two steps:

Preparation of the cationic salt. The cationic (pyrrolidinium/sulfonium/imidazolium) salts were synthesized by the basic compound (*N*-methyl pyrrolidine/diethylsulfide/1-methyl imidazole) with the molar equivalent of an alkyl halide or alkyl tosylate (which was prepared by the tosylation reaction of the corresponding alkyl alcohol with tosyl chloride). It's worth mentioning that the reactivity sequence of the base is 1-methyl imidazole > *N*-methyl pyrrolidine > diethylsulfide.

For 1-methyl imidazole, the general procedure is 1.64g (0.02 mol) of 1-methyl imidazole was dissolved in 5 mL DCM. A molar equivalent of chloromethyl methyl ether/propargyl tosylate was dissolved in 5 mL DCM and added dropwise with an ice-water bath and continued string. Next, the reaction mixture was allowed to rise to room temperature under continuous stirring for 12 h. Then the solvent was removed under vacuum. The product was purified by column chromatography. For *N*-methyl pyrrolidine and diethylsulfide the reaction set-up was similar, but an ice-bath was not used and more vigorous reaction conditions (50–70 °C) were applied. After purification, the products were subjected to the metathesis reaction.

Metathesis reaction. Depending on the anions, different procedures were used for the metathesis reaction. The cation species have little effect on this step. ILs based on PF_6^-, $TFSI^-$ and BF_4^- are all highly hydrophobic. A typical metathesis procedure is 0.01 mol of the salt and the corresponding anionic salt ($NaPF_6$/LiTFSI/$NaBF_4$) (in 1.05 molar equivalent) are dissolved separately in 5 mL DI water. Then the two solutions are mixed and stirred at room temperature for 2 h. The mixture was then extracted with 15 mL DCM. The organic layer was separated and washed with 2 × 5 mL DI water to remove excess $NaPF_6$/LiTFSI/$NaBF_4$. Then the product was dried with anhydrous $MgSO_4$ and decolorized using activated charcoal. Subsequently, the solvent was removed under vacuum. The product was then subjected to high-vacuum (80 °C for 12 h), and 4Å molecular sieves were added to remove traces of moisture.

Dicyanamide (DCA)-based ILs are hydrophilic, so they cannot be prepared by metathesis reaction in water. The following procedure was applied: The precursors (if associated with other anions, such as Br^- and TsO^-) were first converted to Cl^- form by passing through a chloride form ion-exchange resin column. Methanol was used as the mobile phase. The solvent was removed by vacuum distillation after the ion-exchange process. Then the metathesis reaction with NaDCA was carried out as follows—0.02 mol of NaDCA and 0.01 mmol IL (Cl^- form) was added to 30 mL acetone. The mixture was stirred at room temperature for 12 h. Then the solvent was removed under vacuum. The white precipitate (NaCl) formed was filtered. 30 mL of DCM/acetone = 3/1 mixture was added

and stirred for 1 h and filtered again. Anhydrous MgSO4 and activated charcoal were used for drying and decolorization. Subsequently, the solvent was removed under reduced pressure. The residual pale-yellow liquid was DCA-based IL, which was stirred with 4Å molecular sieves to remove traces of moisture.

Py$_{11O1}$ PF$_6$: ^{1}H-NMR (300 MHz, CDCl$_3$): δ (ppm) 4.46 (s, 2H, NCH_2O), 3.60 (s, 3H, OCH_3). 3.67–3.60, 3.50–3.42 (2 sets of m, 4H, CH$_2$CH_2NCH_2CH$_2$), 3.00 (s, 3H, NCH_3), 2.18 (m, 4H, CH$_2$CH_2CH_2CH$_2$). ^{13}C-NMR (300 MHz, CDCl$_3$): δ (ppm) 90.7 (NCH$_2$O), 61.1 (CH$_2$CH$_2$NCH$_2$CH$_2$), 60.0 (OCH$_3$), 47.2 (NCH$_3$), 22.0 (CH$_2$$CH_2$$CH_2CH_2$). Anal. calcd. for C$_7H_{16}F_6$NOP (%): C, 30.55; H, 5.86; N, 5.09. Found: C, 30.43; H, 5.80; N, 5.01.

Py$_{1P}$ TFSI: ^{1}H-NMR (300 MHz, CDCl$_3$): δ (ppm) 4.02 (s, 2H, NCH_2CCH), 3.54–3.50, 3.41–3.38 (2 sets of m, 4H, CH$_2$CH_2NCH_2CH$_2$), 3.03 (s, 3H, CH_3), 2.79 (s, 2H, CCH), 2.12 (m, 4H, CH$_2$CH_2CH_2CH$_2$); ^{13}C-NMR (300 MHz, CDCl$_3$): δ (ppm) 120 (q, J_{CF} = 319 Hz, CF$_3$), 80.6 (CCH), 70.9 (CCH), 63.9 (CH$_2$CH$_2$NCH$_2$CH$_2$), 53.3 (NCH$_2$CCH), 49.4 (CH$_3$), 21.7 (CH$_2$$CH_2$$CH_2CH_2$). Anal. calcd. for C$_{10}H_{14}F_6N_2O_4S_2$ (%): C, 29.70; H, 3.49; N, 6.93; S, 15.86. Found: C, 29.62; H, 3.39; N, 6.93; S, 15.93.

Im$_{14}$ DCA [31]: ^{1}H-NMR (500 MHz, DMSO-d_6): δ (ppm) 9.11 (s, 1H, C2-H), 7.76 (s, 1H, C4/5-H), 7.70 (s, 1H, C4/5-H), 4.16 (t, 2H, NCH_2CH$_2$CH$_2$CH$_3$), 3.85 (s, 3H, NCH_3), 1.76 (quintet, 2H, NCH$_2$CH_2CH$_2$CH$_3$), 1.24 (sextet, 2H, NCH$_2$CH$_2$CH_2CH$_3$), 0.90 (t, 3H, NCH$_2$CH$_2$CH$_2$CH_3). ^{13}C-NMR (125 MHz, DMSO-d_6): δ (ppm) 136.4 (s, C2), 123.5 (s, $C4/5$), 122.1 (s, $C4/5$), 119.0 (s, N-CN), 48.4 (s, NCH$_2$CH$_2$CH$_2$CH$_3$), 35.6 (s, NCH$_3$), 31.2 (s, NCH$_2$$CH_2CH_2CH_3$), 18.6 (s, NCH$_2CH_2$$CH_2CH_3$), 13.1 (s, NCH$_2CH_2CH_2$$CH_3$). Anal. calcd. for C$_{10}H_{15}N_5$ (%):C, 58.51; H, 7.37; N, 34.12. Found: C, 58.42; H, 7.24; N, 34.06.

Im$_{12}$ TFSI [32]: ^{1}H-NMR (300 MHz, Acetone-d_6): δ (ppm) 9.03 (s, 1H), 7.78 (t, 1H, J = 2.2 Hz), 7.71 (t, 1H, J = 2.2 Hz), 4.39 (q, 2H, J = 9.0 Hz), 4.05(s, 3H), 1.56 (t, 3H, J = 9.0 Hz). ^{13}C-NMR (75 MHz, Acetone-d_6,): δ (ppm) 136.52, 124.22, 122.52, 120.62 (q, J_{CF} = 319.9 Hz), 45.22, 36.06, 14.99. Anal. calcd. for C$_8$H$_{11}$F$_6$N$_3$O$_4$S$_2$ (%): C, 24.55; H, 2.83; N, 10.74; S, 16.39. Found: C, 24.44; H, 2.71; N, 10.63; S, 16.31.

Im$_{12}$ BF$_4$ [32]: ^{1}H-NMR (300.4 MHz, C$_6$D$_6$): δ (ppm) 8.39 ppm (s, 1H, C2-H). 7.26 and 7.33 (t, 2 × 1H, C4/5-H), 4.00 (quartet, 2H, NCH_2CH$_3$), 3.69 (s, 3H, NCH_3), 1.22 (t, 3H, NCH$_2$CH_3). Anal. calcd. for C$_6$H$_{11}$BF$_4$N$_2$ (%): C, 36.40; H, 5.60; N, 14.15. Found: C, 36.25; H, 5.51; N, 14.03.

S$_{131O2}$ TFSI: ^{1}H-NMR (300.13 MHz, CDCl$_3$): δ(ppm) 3.81 (t, J_{HH} = 5.1 Hz, 2H, CH$_2$CH_2O), 3.78 (m, J_{HH} = 6.0 Hz, 1H, SCH), 3.49, 3.43 (2 sets of t, J_{HH} = 4.8 Hz, 2H, CH_2CH$_2$O), 3.36 (s, 3H, OCH_3), 2.80 (s, 3H, SCH_3), 1.49, 1.48 (2 sets of d, J_{HH} = 6.6 Hz, 6H, CHCH_3); ^{13}C-NMR (75.47 MHz, CDCl$_3$): δ(ppm) 119.8 (q, J_{CF} = 321 Hz, CF$_3$), 66.5 (CH$_2$$CH_2$O), 59.1 (O$CH_3$), 46.5 (S$C$H), 40.0 ($CH_2CH_2$O), 20.1 (S$CH_3$), 17.1, 16.7 (2 sets, CHCH$_3$). Anal. calcd. for C$_9$H$_{17}$F$_6$NO$_5$S$_3$ (%): C, 25.17; H, 3.99; N, 3.26; S, 22.40. Found: C. 25.10; H, 4.05; N, 3.13; S, 22.31.

S$_{111O2}$ TFSI: ^{1}H-NMR (300.13 MHz, CDCl$_3$): δ(ppm) 3.81 (t, J_{HH} = 4.8 Hz, 2H, CH$_2$CH_2O), 3.46 (t, J_{HH} = 5.1 Hz, 2H, CH_2CH$_2$O), 3.34 (s, 3H, OCH_3), 2.77 (s, 6H, SCH_3); ^{13}C-NMR (75.47 MHz, CDCl$_3$): δ(ppm) 119.6 (q, J_{CF} = 316 Hz, CF$_3$), 66.9 (CH$_2$$CH_2$O), 58.3 (O$CH_3$), 38.1 ($CH_2CH_2$O), 21.7 (S$CH_3$). Anal. calcd. for C$_7H_{13}F_6NO_5S_3$ (%): C, 20.95; H, 3.26; N, 3.49; S, 23.97. Found: C, 20.86; H, 3.15; N, 3.38; S, 23.88.

S$_{123}$ TFSI: ^{1}H-NMR (300.13 MHz, CDCl$_3$): δ(ppm) 3.69 (m, J_{HH} = 6.9, 1H, SCH), 3.30, 3.20 (2 sets of q, J_{HH} = 6.0 Hz, 2H, SCH_2), 2.72 (s, 3H, SCH_3), 1.55, 1.53 (2 sets of d, J_{HH} = 3.9 Hz, 6H, CHCH_3), 1.45 (t, J_{HH} = 7.5 Hz, 3H, CH$_2$CH_3); ^{13}C-NMR (75.47 MHz, CDCl$_3$): δ(ppm) 119.7 (q, J_{CF} = 317 Hz, CF$_3$), 45.5 (SCH), 33.5 (SCH$_2$), 18.2 (SCH$_3$), 17.5, 16.7 (2 sets, CHCH$_3$), 8.6 (CH$_2$$CH_3$). Anal. calcd. for C$_8H_{15}F_6NO_4S_3$ (%): C, 24.06; H, 3.79; N, 3.51; S, 24.09. Found: C, 24.01; H, 3.71; N, 3.43; S, 24.08.

S$_{221O2}$ TFSI: ^{1}H-NMR (300.13 MHz, CDCl$_3$): δ(ppm) 3.79 (t, J_{HH} = 4.8 Hz, 2H, CH$_2$CH_2O), 3.42 (t, J_{HH} = 5.1 Hz, 2H, CH_2CH$_2$O), 3.33 (s, 3H, OCH_3), 3.29 (q, J_{HH} = 7.2 Hz, 4H, CH_2CH$_3$), 1.44 (t, J_{HH} = 7.5 Hz, 6H, CH$_2$CH_3); ^{13}C-NMR (75.47 MHz, CDCl$_3$): δ(ppm) 119.6 (q, J_{CF} = 318 Hz, CF$_3$),

65.6 (CH_2CH_2O), 58.1 (OCH_3), 37.9 (CH_2CH_2O), 32.8 (CH_2CH_3), 8.5 (CH_2CH_3). Anal. calcd. for $C_9H_{17}F_6NO_5S_3$ (%): C, 25.17; H, 3.99; N, 3.26; S, 22.40. Found: C, 25.04; H, 3.82; N, 3.21; S, 22.28.

S₂₂₂ TFSI: ^{1}H-NMR (300.13 MHz, $CDCl_3$): δ(ppm) 3.26 (q, J_{HH} = 7.2 Hz, 6H, CH_2CH$_3$), 1.47 (t, J_{HH} = 7.5 Hz, 9H, CH$_2$CH_3); ^{13}C-NMR (75.47 MHz, $CDCl_3$): δ(ppm) 119.8 (q, J_{CF} = 317 Hz, CF_3), 32.8 (CH_2), 8.5 (CH_3). Anal. calcd. for $C_8H_{15}F_6NO_4S_3$ (%): C, 24.06; H, 3.79; N, 3.51; S, 24.09. Found: C, 23.90; H, 3.62; N, 3.43; S, 24.02.

S₁₂₁O₂ TFSI: ^{1}H-NMR (300.13 MHz, $CDCl_3$): δ(ppm) 3.80 (t, J_{HH} = 5.4 Hz, 2H, CH$_2$CH_2O), 3.46, 3.42 (2 sets of t, J_{HH} = 5.1 Hz, 2H, CH_2CH$_2$O), 3.36 (s, 3H, OCH_3), 3.30, 3.25 (2 sets of q, J_{HH} = 7.2 Hz, 2H, CH_2CH$_3$), 2.80 (s, 3H, SCH_3), 1.45 (t, J_{HH} = 7.5 Hz, 3H, CH$_2$CH_3); ^{13}C-NMR (75.47 MHz, $CDCl_3$): δ(ppm) 119.5 (q, J_{CF} = 320 Hz, CF_3), 66.5 (CH_2CH_2O), 58.5 (OCH_3), 40.6 (CH_2CH_2O), 33.2 (CH_2CH_3), 22.1 (SCH_3), 8.5 (CH_2CH_3). Anal. calcd. for $C_8H_{15}F_6NO_5S_3$ (%): C, 23.13; H, 3.64; N, 3.37; S, 23.16. Found: C, 23.04; H, 3.43; N, 3.25; S.23.10.

S₁₁₁O₂ DCA: ^{1}H-NMR (300.13 MHz, D_2O): δ(ppm) 3.83 (t, J_{HH} = 5.4 Hz, 2H, CH$_2$CH_2O), 3.45 (t, J_{HH} = 5.1 Hz, 2H, CH_2CH$_2$O), 3.35 (s, 3H, OCH_3), 2.80 (s, 6H, SCH_3); ^{13}C-NMR (75.47 MHz, D_2O): 66.5 (CH_2CH_2O), 58.6 (OCH_3), 38.5 (CH_2CH_2O), 21.5 (SCH_3). N$^-$(CN)$_2$ not observed. Anal. calcd. for $C_7H_{13}N_3OS$ (%): C, 51.86; H, 8.16; N, 22.68; S, 17.31. Found: C, 51.79; H, 8.07; N, 22.72; S, 17.23.

S₂₂₁O₂ DCA: ^{1}H-NMR (300.13 MHz, D_2O): δ(ppm) 3.83 (t, J_{HH} = 5.4 Hz, 2H, CH$_2$CH_2O), 3.45 (t, J_{HH} = 5.1 Hz, 2H, CH_2CH$_2$O), 3.35 (s, 3H, OCH_3), 3.31 (q, J_{HH} = 7.2 Hz, 4H, CH_2CH$_3$), 1.38 (t, J_{HH} = 7.5 Hz, 6H, CH$_2$CH_3); ^{13}C-NMR (75.47 MHz, D_2O): 66.0 (CH_2CH_2O), 58.5 (OCH_3), 38.4 (CH_2CH_2O), 33.5 (CH_2CH_3), 7.9 (CH_2CH_3). N$^-$(CN)$_2$ not observed. Anal. calcd. for $C_9H_{17}N_3OS$ (%): C, 50.20; H, 7.96; N, 19.52; S, 14.89. Found: C, 50.04; H, 7.82; N, 19.43; S, 14.78.

S₂₂₂ DCA: ^{1}H-NMR (300.13 MHz, D_2O): δ(ppm) 3.16 (q, J_{HH} = 7.5 Hz, 6H, CH_2CH$_3$), 1.37 (t, J_{HH} = 7.5 Hz, 9H, CH$_2$CH_3); ^{13}C-NMR (75.47 MHz, D_2O): δ(ppm) 33.5 (CH_2), 7.9 (CH_3). N$^-$(CN)$_2$ not observed. Anal. calcd. for $C_8H_{15}N_3S$ (%): C, 51.86; H, 8.16; N, 22.68; S, 17.31. Found: C, 51.75, H, 8.11; N, 22.57; S, 17.24.

2.3. Synthesis of New ZILs

N-methyl diethanoxycyanoethyl amine (NMDE-CN)—2.22 g (18.61 mmol) of *N*-methyldiethanolamine and 2.73 g (51.51 mmol) of acrylonitrile were placed in a 50 mL flask in an ice water bath and stirred. 0.7 mL of TMAH was added drop wise to the mixture. 0.1 M HCl solution was added to the mixture after one day reaction at room temperature (RT). After extracting (3×) with dichloromethane (DCM), the solution was filtered through a silica gel column using diethyl ether and DCM (1:1) as the eluent. The solvent was rotavaped and the product was dried under high vacuum at 60 °C. FTIR: Nitrile group (-CN) stretching absorption at 2242.2 cm^{-1}, no alcohol group (-OH) stretching absorption at ~3500 cm^{-1}. ^{1}H-NMR (300 MHz, $CDCl_3$): δ 3.7 (t), 3.5 (t), 2.6 (t), 2.3 (s) ppm. Anal. calcd. for $C_{11}H_{19}N_3O_2$ (%): C, 58.64; H, 8.50; N, 18.65. Found: C, 58.93; H, 8.44; N, 18.46.

Synthesis of NMDE-ZIL—0.8524 g of NMDE-CN, 0.6124 g of 1,3-propane sultone and 5 mL of acetonitrile were placed in a flask. The solution was stirred for overnight at RT. After the reaction was done, acetonitrile was removed by rotavap. Tetrahydrofuran (THF) was used to wash out the excess sultone. The pure product was obtained after the solvent was removed. Anal. calcd. for $C_{14}H_{25}N_3O_5S$ (%): C, 48.40; H, 7.25; N, 12.09; S, 9.23. Found: C, 48.27; H, 7.17; N, 11.90; S, 9.07.

Synthesis of 2-cyanoethyl 2-ethoxy 2-ethoxy N, N-methyl amine (DAEE-CN)—2.28 g of DAEE and 1.46 g of acrylonitrile were placed in a 50 mL flask in an ice water bath and stirred. About 0.3 mL of TMAH was added drop wise to the mixture. 5.5 mL of 0.1 M HCl solution was added to the mixture after one day reaction at RT. After extracting (3×) by DCM, the solution was filtered through silica gel using diethyl ether and DCM (4:1) as the eluent. The solvent was rotavaped and the product was dried under high vacuum at 60 °C. FTIR: Nitrile group (-CN) stretching absorption at 2250.0 cm^{-1},

no alcohol group (-OH) stretching absorption at ~3500 cm^{-1}. ^{1}H-NMR (300 MHz, CDCl$_3$): δ 3.6 (m), 2.5 (t), 2.4 (t), 2.2 (s) ppm. Anal. calcd. for C$_9$H$_{18}$N$_2$O$_2$ (%): C, 58.04; H, 9.74; N, 15.04. Found: C, 58.08; H, 9.55; N, 15.01.

Synthesis of DAEE-ZIL—0.65 g of DAEE-CN, 0.51 g of 1,3-propane sultone and 5 mL of acetonitrile were placed in a flask. The solution was stirred overnight at RT. After the reaction was done, acetonitrile was removed by rotavap. THF was used to wash out the excess sultone. The pure product was obtained after the solvent was removed. Anal. calcd. for C$_{12}$H$_{24}$N$_2$O$_5$S (%): C, 46.74; H, 7.84; N, 9.08; S, 10.40. Found: C, 46.59; H, 7.72; N, 9.01; S, 10.21.

Synthesis of TBAE-CN—3.15 g of 2-*tert*-butylamino ethanol, 5.78 of acrylonitrile and 2 mL of water were placed in a 50 mL flask in an ice water bath and stirred. 0.8 mL of TMAH was added drop-wise to the mixture. 0.1 M HCl solution was added to the solution after one day reaction. The product was obtained after the similar purification procedure described above for DAEE-CN. FTIR: Nitrile group (-CN) stretching absorption at 2250.3 cm^{-1}, no alcohol group (-OH) stretching absorption at ~3500 cm^{-1}. ^{1}H-NMR (300 MHz, CDCl$_3$): δ 3.6 (t), 3.4 (t), 2.7 (t), 2.6 (t), 1.0 (s) ppm. Anal. calcd. for C$_{12}$H$_{21}$N$_3$O (%): C, 64.54; H, 9.48; N, 18.82. Found: C, 64.41; H, 9.66; N, 18.72.

Synthesis of TBAE-ZIL: 1.68 g of TBAE-CN, 1.17 g of 1,3-propane sultone and 7 mL of acetonitrile were placed in a flask. The solution was stirred for overnight at RT. The pure product was obtained after the similar purification procedure described above for DAEE-CN. Anal. calcd. for C$_{15}$H$_{27}$N$_3$O$_4$S (%): C, 46.74; H, 7.84; N, 9.08; S, 10.40. Found: C, 46.66; H, 7.72; N, 9.02; S, 10.31.

Synthesis of TEA-CN: 1.55 g of triethanolamine, 2.87 g of acrylonitrile and 2 mL water were placed in a 50 mL flask in an ice water bath and stirred. 0.4 mL of TMAH was added drop wise to the solution. After two days reaction time, 0.1 M HCl solution was added to the mixture. The purification procedure was similar as described above for DAEE-CN. FTIR: Nitrile group (-CN) stretching absorption at 2250.3 cm^{-1}, no alcohol group (-OH) stretching absorption at ~3500 cm^{-1}. ^{1}H-NMR (300 MHz, CDCl$_3$): δ 3.6 (t), 3.4 (t), 2.7 (t), 2.6 (t), 1.0 (s) ppm. Anal. calcd. for C$_{15}$H$_{24}$N$_4$O$_3$ (%): C, 58.42; H, 7.84; N, 18.17. Found: C, 58.31; H, 7.65; N, 18.10.

Synthesis of TEA-ZIL: 1.08 g of TBAE-CN, 0.51 g of 1,3-propane sultone and 4 mL of acetonitrile were placed in a flask. The solution was stirred for overnight at room temperature. The pure product was obtained after the similar purification procedure as described above for DAEE-CN. Anal. calcd. for C$_{18}$H$_{30}$N$_4$O$_6$S (%): C, 50.22; H, 7.02; N, 13.01; S, 7.45. Found: C, 50.09; H, 7.12; N, 12.92; S, 7.36.

2.4. Viscosity Measurement

The dynamic viscosity of all ILs was measured using a Brookfield DV3T viscometer containing spindle CPA-40Z. A schematic of the experimental set-up is depicted in Figure 1. A recirculating chiller (Isotemp 1013S, Fisher Scientific, Hampton, NH, USA) was linked with the heating container of the viscometer to keep the temperature of the sample chamber stable at 25 (±0.1) °C by water/glycol = 1/1 liquid cycling. The instrument was calibrated with a mineral oil viscosity standard fluid (B29) supplied by the manufacturer. All samples were dried with 4 Å molecular sieves for 2 days to remove any possible moisture prior to the viscosity measurement. A sample of about 0.5 mL was kept in the sample chamber for ~10 min prior to acquiring the viscosity data.

2.5. Ionic Conductivity Measurement

The ionic conductivity was measured using a Mettler Toledo S230-Kit conductivity meter (Metler Toledo, Columbus, OH, USA) in an environmental chamber from 25 °C to 70 °C [33]. The conductivity meter was calibrated against a standard (0.01 mol L^{-1} KCl aqueous solution) with an ionic conductivity of 1.314 mS cm^{-1} at 25.0 °C.
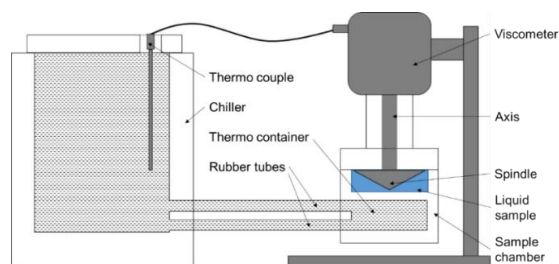
Figure 1. A schematic of the viscosity measurement set-up.

2.6. Flammability Test

We carried out a flammability test called self-extinguishing time (SET) in accordance with a reported study [34]. Each electrolyte was tested three times: The burner was ignited above the sample for 5 s and then switched off. The ignition time after flame setting and the self-extinguish time after removing the burner were measured as an indicator of the nonflammability index of the sample [35]. The time it took for the flame to extinguish was normalized against liquid mass to give the SET in second/gram [36]. The electrolyte was judged to be nonflammable if the electrolyte never ignited during the testing, or if the ignition of electrolyte ceased when the flame was removed [37].

2.7. Fabrication of EDLC Coin Cells and Electrochemical Measurements

Fabrication of coin cells. The electrode slurry was prepared by mixing 90 wt.% mesoporous carbon and 10 wt.% carboxymethyl cellulose (CMC) binder in a 50% water/ethanol solution. The slurry was cast onto an aluminum foil substrate and then dried at 60 °C for 24 h. The AC-coated aluminum foil was punched to obtain electrode discs, each containing ~1.8 mg (±0.1 mg) electrode material. CR2032-type coin cells were assembled in an Ar-filled glove box with oxygen content less than 1 ppm. The cells contained Celgard 2535 as the separator and symmetric electrodes.

Cyclic voltammetry (CV). The test was performed on a PARSTAT 4000A Potentiostat Galvanostat instrument (Ametek SI, Oak Ridge, TN, USA). Two-electrode test cells were initially charged from the open circuit voltage to the maximum voltage (2.50 V to 3.50 V, gradually increased by 0.25 V per test), and then the voltage was switched between 0 and the maximum at a scan rate of 10 mV s^{-1}.

Electrical impedance spectroscopy (EIS). The inner resistance of our EDLC cells was measured from EIS and Nyquist plot curves. Data were collected using the same CV instrument described above. The frequency range of the discharge state of the cells was recorded between 0.1 MHz and 1 Hz, with an amplitude of 10 mV.

Cycling performance. The cycling performance of the cell was tested in an MTI battery analyzer (BST8-WA). Coin cells with 6 different formulations ran 50 charge-discharge cycles at 0.5, 1.0, 2.0 and 4.0 A g^{-1}, respectively. Then 4000-cycle long-term cycling test was applied using the best two electrolytes.

3. Results and Discussion

3.1. Synthesis and Properties of Specifically Designed ILs

ILs possess a wide range of viscosities ranging from 15 to 40,000 cP, compared to viscosities of typical organic solvents which range from 0.2 to 100 cP. Since ionic conductivity is inversely related to viscosity, most ILs fall short of electrolyte applications [38,39]. Among the ILs studied for electrolyte applications, pyrrolidinium (Py), imidazolium (Im), and sulfonium (S) cations with TFSI as the anion display reasonably low viscosity [9,13–16]. Consequently, they are attractive in terms of achieving the target electrolyte properties, viz., ionic conductivity (>7 mS cm^{-1}). Several ILs display very good pristine ionic conductivity, but they are not suitable for Li-ion battery electrolytes because of their poor lithium salt (LiTFSI) dissolution and/or a dramatic drop in ionic conductivity, due to a sharp rise in viscosity after adding the Li-salt. Consequently, the preparation of IL-based electrolytes containing at

least 0.5 M LiTFSI with ionic conductivity in excess of 7 mS cm^{-1} is very challenging. In this study, we have addressed two questions. Which class of ILs has the best chance of meeting basic ionic conductivity requirements? What structural modifications would achieve Li-salt dissolution in excess of 0.5 M? To answer these questions, we have synthesized many new ILs to draw structure-property relationships. Tables 1, 2 and 6 list the structures of ILs synthesized. The major emphasis was given on ether group-containing ILs because we reason that the ether group will effectively coordinate with the lithium salt, leading to improved lithium salt dissolution. We have also synthesized several previously reported ILs which are not commercially available to compare properties with our new ILs.

Table 1. Properties of Pyrrolidinium-based ionic liquids (ILs).

Abbreviation	Structure	Molecular Weight (g mol^{-1})	Viscosity (cP)	Ionic Conductivity (mS cm^{-1}) (25 °C)	Comments
Py$_{11O1}$ FSI		310.34	25.5 (28.5)	11.5 (10.3)	Not commercially available [40]
Py$_{11O1}$ TFSI		410.04	37.8 (40)	5.4 (5.5)	Not commercially available [41]
Py$_{11O1}$ BF$_4$		217.01	62.3 (100)	7.9 (6.8)	Not commercially available [41]
Py$_{1P}$ TFSI		404.35	91.1	2.6	*New compound*
Py$_{1A}$ TFSI		406.37	48.7 (52)	5.1 (3.7)	Not commercially available [42,43]
Py$_{13}$ TFSI		408.38	60	3.8	Not commercially available [44,45]

Number in ( ) represents literature value.

Table 2. Properties of Imidazolinium-based ILs.

Abbreviation	Structure	Molecular Weight (g mol^{-1})	Viscosity (cP)	Ionic Conductivity (mS cm^{-1}) (25 °C)	Comments
Im$_{14}$ DCA		205.26	31.8	10.5	Commercially available [45–47]
Im$_{11O2}$ TFSI		407.31	48.5	3.6	Not commercially available [48,49]
Im$_{12O2}$ TFSI		421.34	45.1	3.3	Not commercially available [49,50]
Im$_{12}$ TFSI		391.31	33.3	7.1	Commercially available [48,51]
Im$_{12}$ BF$_4$		198.10	36.0	15.2	Commercially available [51–53]
Im$_{12}$ DCA		177.21	14.8	26.3	Not commercially available [54]

Figures 2–4 describe the synthetic strategy to our new ILs. As mentioned in the experimental section, the synthesis of TFSI-based ILs is straightforward and involves two steps: Preparation of an appropriate cationic salt (typically chloride and bromide) followed by an aqueous metathesis reaction with LiTFSI [43]. Since all TFSI-based ILs are insoluble in water, the metathesis product separates as an organic layer. By contrast, the synthesis of DCA-based ILs is rather complicated. The complicacy arises, due to the high solubility of DCA-based ILs in water. Traditionally, the DCA-based ILs have been prepared via the metathesis reaction of a cationic iodide salt with AgDCA in a polar solvent (such as methanol or acetone). This is due to the extremely low solubility of AgI, which precipitates out of the solution [57–61]. There are two major disadvantages to this methodology. First, the desired iodo compound is not always commercially available. Second, AgDCA is very expensive as it must be prepared by the metathesis reaction between two rather expensive salts, $AgNO_3$ and NaDCA. Our synthetic strategy to prepare DCA-based ILs is very different from the literature [43]. As depicted in Figure 3, our strategy involves an ion-exchange resin and is based on the fact that NaCl possesses much lower solubility than NaDCA in acetone. The solubility of NaCl is reported as 4.2×10^{-5} g per 100 g acetone at 25 °C [62]. Another notable advantage of our method is that the procedure does not require the preparation of the iodo compounds. Additionally, the ion-exchange resin can be reused multiple times simply by regeneration with HCl solution. All new ILs were characterized by ^{1}H-NMR, ^{13}C-NMR and elemental analysis.
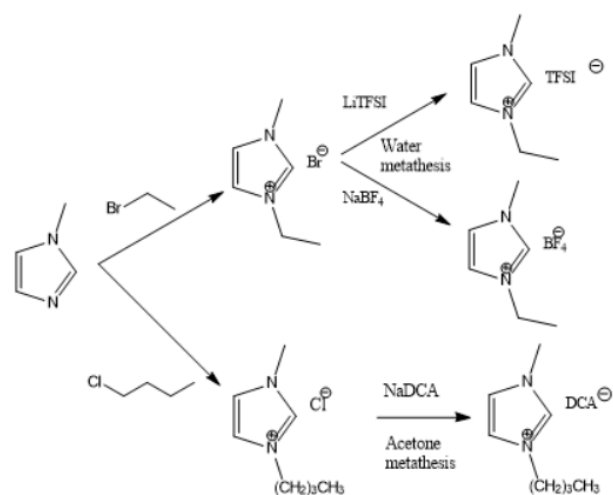
Figure 2. Synthetic strategy to imidazolium ILs.
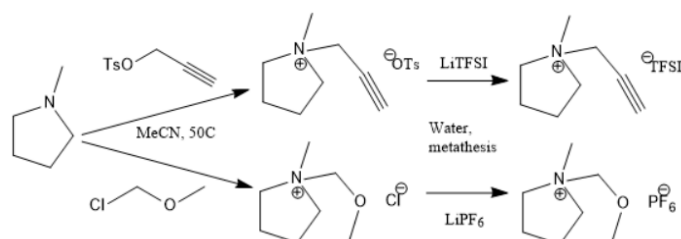
Figure 3. Synthetic strategy to pyrrolidinium ILs.

Tables 1, 2 and 6 list viscosity and ionic conductivity values of the ILs synthesized. Surprisingly, ether group-containing ILs displayed better ionic conductivity when compared with the corresponding alkyl analog (e.g., Py_{11O1} TFSI vs. Py_{13} TFSI). DCA anion-based ILs are the best when it comes to both low viscosity and high ionic conductivity. Among the hydrocarbon substituted ILs, allyl group containing ILs displayed superior properties than alkyl or alkyne group containing ILs (e.g., Py_{1A} TFSI vs. Py_{1P} TFSI and Py_{13} TFSI). In general, sulfonium-based ILs display low viscosity, but it did not translate to high ionic conductivity for most compounds except for S_{221O2} DCA (new ether

group-containing compound), which displayed remarkably low viscosity (25.3 cP) and high ionic conductivity (11.6 mS cm^{-1}). We have also identified two ILs with outstanding properties, Im$_{12}$ DCA (viscosity, 14.8 cP and ionic conductivity, 26.3 mS cm^{-1}) and S$_{222}$ DCA (viscosity, 14.4 cP and ionic conductivity, 26.9 mS cm^{-1}). Although their Li-salt dissolution power is very poor, we believe that they can be used as a thinner solvent to improve the properties of our new ether group-containing ILs (*vide infra*).
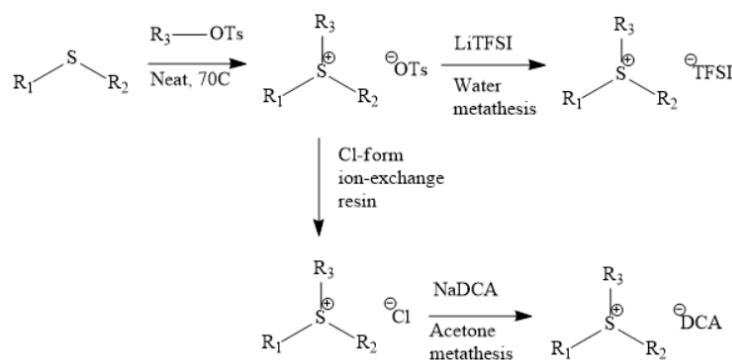
Figure 4. Improved synthetic strategy to prepare DCA-based ILs [33].

3.2. Synthesis and Properties of Specifically Designed FILs

In the past decades, a number of FILs (ILs with fluorine-containing cations) have been synthesized [63,64]. While they have been tested for anti-fungal drugs [65], enhanced oxygen solubility [66], photovoltaics [67], surfactants [68], and super hydrophobic coatings [69], their applicability for Li-ion battery electrolytes have not been explored. Fluorine-containing electrolyte solvents possess several attractive features. A key feature is that they are known to form stable solid electrolyte interphase (SEI) on the anode surface, leading to superior cell stability [70]. Other special attributes of fluorinated solvents include superior flame-retardant properties [71]; reduction of boiling temperature and generally lower viscosity [72]. Additionally, the influence of inter-ion hydrogen bonding can be diminished by introducing fluorine-containing groups into the IL cation—especially when employing TFSI as the counter anion [73]. In view of these considerations, we believe that through the combination of a fluorinated functional group (e.g., -CF$_3$) and ethylene oxide (EO) moiety (-CH$_2$CH$_2$O-) in the cation, ILs may be produced that will display non-volatility, non-flammability, low viscosities and high ionic conductivities. As mentioned earlier, the EO unit is known as one of the best solvating mediums for lithium salts [74]. The EO unit provides a suitable space for Li-ion to coordinate with oxygen, and Li-ion migration is associated with the segmental mobility of the EO moiety [75]. Furthermore, a reduction of the symmetry, introduced by the presence of the EO functionality, may cause a melting point depression. This is attributed to a reduction in anion-cation interaction resulting from asymmetry and a delocalized charge. Moreover, as mentioned above, the asymmetric structure could increase the lithium ion transport, and hence ionic conductivity. With these attributes of FILs in mind, our research group has synthesized several new FILs [33]. The structures and properties of some of the best FILs are presented in Table 3. We are pleased to report that fluoro analogs possess similar viscosity, but displayed higher ionic conductivity. This trend is very prominent in Im$_{12O2}$ TFSI (viscosity, 45.1 cP and ionic conductivity, 3.3) and Im$_{1TFO2}$ TFSI (viscosity, 49.8 cP and ionic conductivity, 5.3) analogs. The DCA-based FILs demonstrated superior viscosity values in comparison to TFSI-based FILs.

Table 3. Properties of fluorine-containing ionic liquids (FILs).

Abbreviation	Structure	Molecular Weight (g mol^{-1})	Viscosity (cP)	Ionic Conductivity (mS cm^{-1}) (25 °C)	Comments
P$_{y1TFO2}$ DCA		278.27	60.6	1.2	*New compound* [33]
P$_{y1TFO2}$ TFSI		492.38	78.9	2.3	*New compound* [33]
Im$_{1TFO2}$ DCA		274.34	17.32	3.6	*New compound* [33]
Im$_{1TFO2}$ TFSI		488.35	49.8	5.3	*New compound* [33]
S$_{22TFO2}$ DCA		283.31	27.6	5.2	*New compound* [33]
S$_{22TFO2}$ TFSI		497.42	39.0	2.2	*New compound* [33]
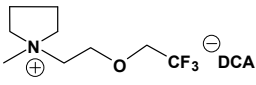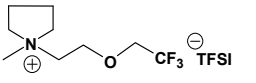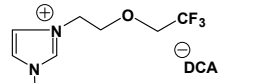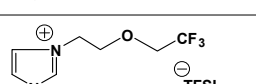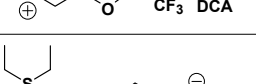
As can be inferred from the data presented in Table 3, the FILs are unlikely to serve as a single solvent system for the electrolyte application, since their pristine ionic conductivity is already below the electrolyte requirement (>7 mS cm^{-1}) and expected to be much lower when Li-salt will be added. Therefore, viscosity manipulation is the best way to resolve this issue. Earlier we mentioned two low molecular weight ILs, Im$_{12}$ DCA and S$_{222}$ DCA, with attractive viscosity and ionic conductivity values. We believe these ILs as a co-solvent ("thinner") may boost the ionic conductivities of the FIL-based electrolytes. Accordingly, we have prepared several electrolyte formulations using Im$_{12}$ DCA as the thinner solvent with the best member of Py, Im and S-cation-based FILs. We made the electrolytes in a way that all electrolytes possess 0.5 M concentration of LiTFSI in 1:1 wt.% FIL/Thinner (Table 4). We were delighted to observe that all formulated electrolytes showed outstanding ionic conductivity at room temperature (similar to commercial carbonate-based Li-ion battery electrolytes, ~11 mS cm^{-1}). At high temperatures, they were outstanding too. To our knowledge, these are the first examples of LiTFSI salt containing all IL-based electrolytes (i.e., no organic solvents) that displayed ionic conductivity in excess of 10 mS cm^{-1}.

Table 4. Properties of FIL-based formulated electrolytes containing 0.5 M LiTFSI [33].

Electrolyte	FIL	Component Weight (g)			Ionic Conductivity (mS cm^{-1})	
		FIL	Im$_{12}$ DCA	LiTFSI	25 °C	70 °C
Ea1	P$_{y1TFO2}$ DCA	0.1002	0.1007	0.0233	10.0	29.6
Ea3	P$_{y1TFO2}$ TFSI	0.0999	0.1001	0.0216	9.7	24.6
Eb1	Im$_{1TFO2}$ DCA	0.1014	0.1007	0.0236	9.1	30.8
Eb3	Im$_{1TFO2}$ TFSI	0.1007	0.1005	0.0215	10.5	29.3
Ec1	S$_{22TFO2}$ DCA	0.1012	0.1010	0.0245	9.1	25.0
Ec3	S$_{22TFO2}$ TFSI	0.1008	0.1006	0.0227	7.9	22.8

Having been encouraged by the ionic conductivity data, we tested the nonflammability behavior of these electrolytes. This property is very important as the carbonate-based electrolytes are highly flammable and known to catch fire under abusive conditions. In order to investigate the flammable behavior of the formulated electrolytes we carried out a flammability test called self-extinguishing time

(SET) [34–37]. The details of the test are described in the experimental section. It is clearly observed from Figure 5 that all the three series of electrolytes may be certified as nonflammable, since they cannot be ignited, meaning their SET is measured to be 0s. We also confirmed that neat FILs were completely nonflammable in nature, thus contributing to the high safety of the formulated electrolyte systems.
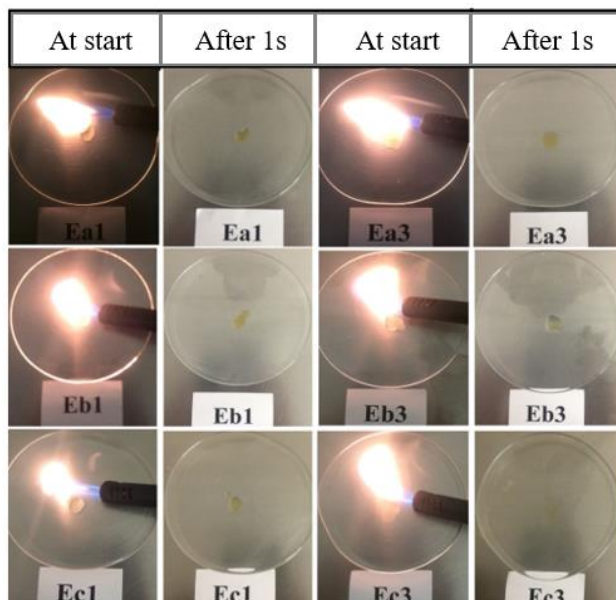
Figure 5. Development of the flames for different formulated electrolytes during the self-extinguishing time (SET) test directly at the burner was turned on (at the start) and was turned off (after 1 s), respectively (see Table 4 for the sample/formulation number) [33].

3.3. Synthesis and Properties of Specifically Designed DILs

Dicationic ionic liquids (DILs) consist of an anion and a doubly charged cation, which is composed of two singly charged cations as head groups linked by a variable length of alkyl or oligo ethylene glycol (OEG) chain as a rigid or flexible spacer. Thus, the DILs can offer the opportunity to investigate both the influence of cation and anion variation, and the influence of the chain length. While currently most research groups have been focusing on mono cationic-type ILs, the number of publications on DILs has been steadily increasing [76,77]. Anderson et al. presented the synthesis and characterization of a variety of DILs containing hydrocarbon spacers [78]. Kubisa and Biedron investigated DILs obtained by functionalization of OEG with triphenylphosphine [79]. However, the relationship studies between the structure and physicochemical characteristics are still rare. Therefore, it is worthwhile to investigate other new DIL structures to gain further understanding and extend the applications of DILs as electrolyte components. Recently, we reported several new OEG-spacer containing DILs [54]. Our hypothesis was that DILs should have the capability to dissolve more lithium salts in order to have higher Li^+ conductivity, if DILs are intended to be applied in Li-ion batteries. Thus, by incorporating an OEG segment into the DILs structure, the conductivity could be enhanced primarily by improving cation transport through the OEG segment. Table 5 depicts the structures and properties of some of the high performing DILs. It is important to note that DILs with shorter EO segments (<4) were not as good as EO = 4 in terms of ionic conductivity [54].

Table 5. Properties of dicationic ionic liquids (DILs).

Abbreviation	Structure	Molecular Weight (g mol^{-1})	Viscosity (cP)	Ionic Conductivity (mS cm^{-1}) (25 °C)	Comments
DP$_{y1}$4O DCA		506.64	49.5	1.5	*New compound* [54]
DP$_{y1}$4O TFSI		934.85	189.6	1.0	*New compound* [54]
DIm$_4$4O DCA		584.71	75.3	1.4	*New compound* [54]
DIm$_4$4O TFSI		1012.92	298.6	0.7	*New compound* [54]
DS$_{22}$4O DCA		516.72	85.2	3.4	*New compound* [54]
DS$_{22}$4O TFSI		944.93	110.4	2.4	*New compound* [54]

Table 6. Properties of Sulfonium-based ILs.

Abbreviation	Structure	Molecular Weight (g mol^{-1})	Viscosity (cP)	Ionic Conductivity (mS cm^{-1}) (25 °C)	Comments
S$_{131O2}$ TFSI		429.42	38.9	2.7	*New compound*
S$_{111O2}$ TFSI		401.37	47 (46.8)	3.8 (3.9)	Not commercially available [55]
S$_{123}$ TFSI		399.40	39.3	4.4	*New compound*
S$_{221O2}$ TFSI		429.42	33.0	4.1	*New compound*
S$_{222}$ TFSI		399.40	30.5 (33.7)	5.6 (7.3)	Commercially available [56]
S$_{121O2}$ TFSI		415.40	34.5 (30.8)	3.9 (4.9)	Not commercially available [56]
S$_{111O2}$ DCA		187.26	41.8	5.0	*New compound*
S$_{221O2}$ DCA		215.31	25.3	11.6	*New compound*
S$_{222}$ DCA		185.29	14.4	26.9	Not commercially available [57]

Number in ( ) represents literature value.

As expected, DILs displayed very high viscosity resulting in low pristine ionic conductivity. However, the dissolution of LiTFSI in these DILs was excellent. This prompted us to study electrolytic properties of formulated electrolytes using Im$_{12}$ DCA as the thinner IL co-solvent. In general, the properties of the DIL-formulated electrolytes showed slightly inferior to FIL-based electrolytes

(Table 7). Two electrolyte formulations that passed the minimum ionic conductivity threshold are DIm_{44O} TFSI and DS_{224O} DCA.

Table 7. Properties of DIL-based formulated electrolytes containing 0.5 M LiTFSI [54].

Electrolyte	DIL	Component Weight (g)			Ionic Conductivity (mS cm^{-1})	
		DIL	Im_{12} DCA	LiTFSI	25 °C	70 °C
E4a	$DP_{y1}4O$ DCA	0.0995	0.1002	0.0240	3.7	15.2
E8a	$DP_{y1}4O$ TFSI	0.1022	0.1002	0.0215	4.7	16.4
E4b	DIm_4O DCA	0.1020	0.1002	0.0244	4.8	17.0
E8b	DIm_4O TFSI	0.1024	0.1006	0.0218	8.4	20.8
E4c	$DS_{22}4O$ DCA	0.1017	0.1001	0.0242	8.2	22.7
E8c	$DS_{22}4O$ TFSI	0.1012	0.1003	0.0219	6.8	24.3

Similar to the FIL-based electrolytes, we studied the nonflammable properties of these DIL-based electrolytes. It is apparent from Figure 6 that all three series of electrolytes may be certified to be nonflammable, as they could not be ignited, meaning their SETs are measured to be zero. We also confirmed that neat DILs were completely nonflammable in nature, thus contributing to the high safety of the resulting electrolytes.
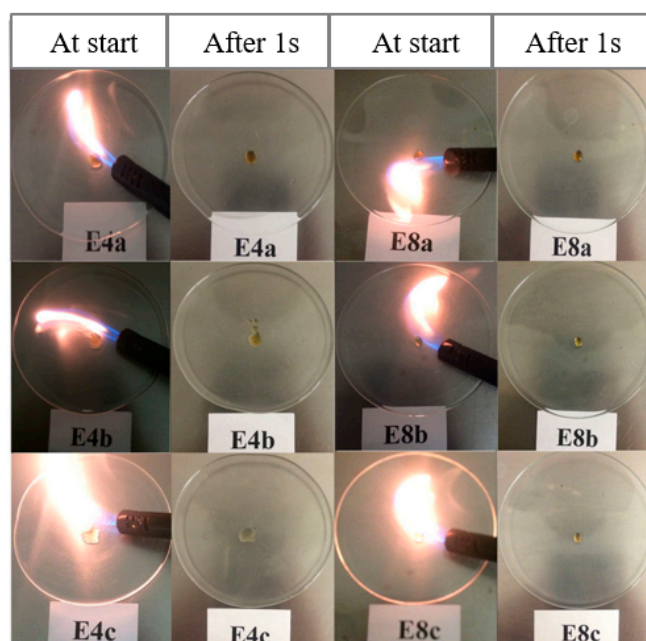
Figure 6. Development of the flames for different DIL-based electrolytes during SET test directly at the burner was turned on (at the start) and was turned off (after 1 s), respectively [54].

3.4. Synthesis and Properties of Specifically Designed ZILs

Zwitterionic liquids (ZILs), a unique class of ILs, possess a high dielectric constant, due to the presence of two permanent opposite charges connected by covalent bonds in the same molecule. ZILs are also nonvolatile and exhibit thermal and electrochemical properties similar to that of ILs [80]. It has been reported that ZILs derived from ammonium, pyrrolidinium, or imidazolium cations significantly promote dissociation of lithium ions [81,82], and consequently, dissolve more lithium salts (in excess of 1 M) compared to traditional ILs. However, similar to ILs, ZILs are also very viscous, leading to low pristine ionic conductivity. This single issue calls for a formulation of ILs with a suitable thinner solvent.

In this study, we have synthesized four new specifically designed ZILs: NMDE-ZIL, DAEE-ZIL, TBAE-ZIL and TEA-ZIL. We introduced two specific features (nitrile and ether groups) in these

molecules to address the issues of ionic conductivity and Li-salt dissolution. A high dielectric constant of an electrolyte solvent is crucial in order to achieve high ionic conductivity because a high dielectric constant promotes superior ion dissociation. The incorporation of polar nitrile groups in the ZIL materials is a direct response to this issue. The lack of adequate Li-salt dissolution in ILs has been another critical issue. Similar to FILs and DILs, we reason that this issue can be best addressed by introducing ether moieties, which chelate effectively with Li^+ and facilitate the lithium ions to be structurally transferred between two ligands.

The synthesis of new ZILs requires nitrile and ether groups substituted with quaternary amines. This objective was accomplished in one step by the Michael addition reaction between a hydroxyl group containing a tertiary amine and acrylonitrile in almost quantitative yield (Figures 7–10). In a recent study, we have published a series of nitrile-groups containing polyether solvents for LIB electrolytes by this strategy [83].
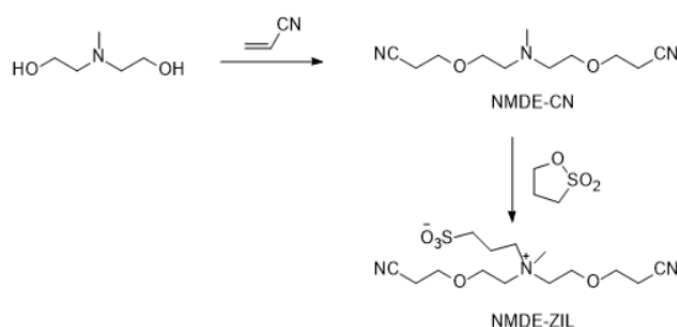
Figure 7. Synthesis of NMDE-ZIL.
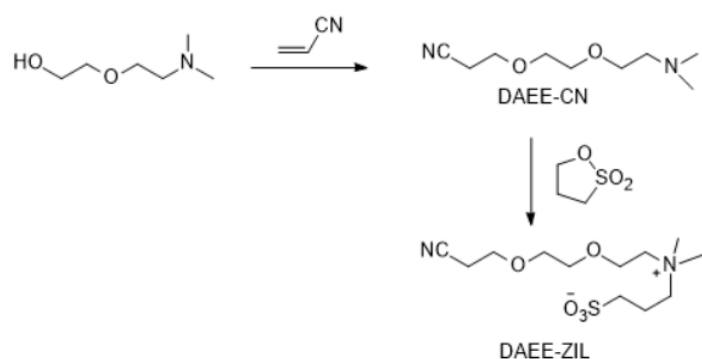
Figure 8. Synthesis of DAEE-ZIL.
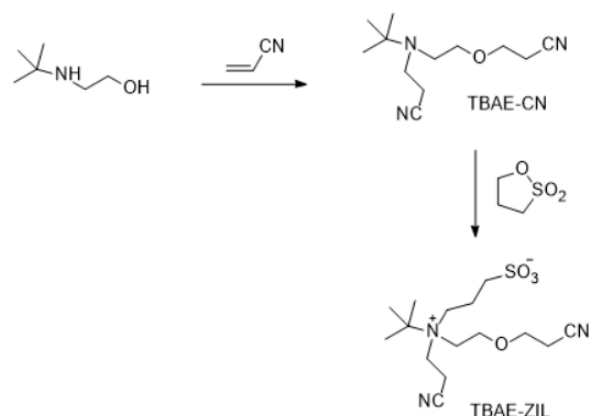
Figure 9. Synthesis of TBAE-ZIL.
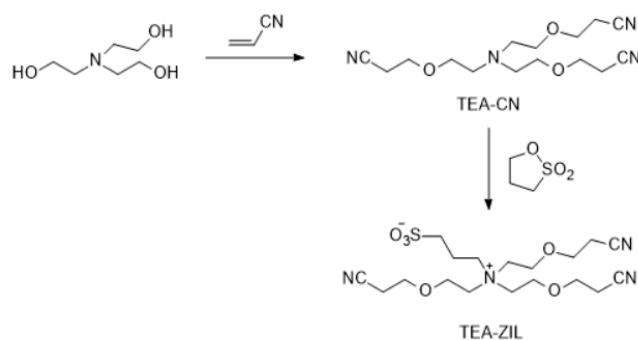
Figure 10. Synthesis of TEA-ZIL.

Unlike the aforementioned FILs and DILs, these ZILs are highly viscous or semi-solids, and not compatible with Im_{12} DCA thinner IL co-solvent. Thus, a suitable organic solvent is needed for electrolyte formulations. In order to compensate high viscosity and low conductivity of ILs, several organic co-solvents, viz., ethylene carbonate (EC), propylene carbonate (PC), vinylene carbonate (VC), fluoroethylene carbonate (FEC), ethylene sulfite (ES), gamma-butyrolactone (γ-BL), fluoroether (FET) and adiponitrile (ADN) have been investigated [84–88]. Unfortunately, none of these solvents was found to be compatible with these ZILs. The only solvent found to be very promising was 2-nitropropane (2-NP), which possesses a very good dielectric constant (25.2), low viscosity (0.72 cP), and the relatively high boiling point when compared to DMC (120 °C vs. 90 °C). Table 8 summarizes the electrolyte formulations prepared in this study. Different concentrations of the lithium salt and the effect of weight ratios of ZIL/2-NP were studied for achieving superior ionic conductivity. We were pleased to see the very high Li-salt dissolution power (in excess of 2 M) of the ZIL/2-NP solvent mixtures.

Table 8. Electrolyte formulations investigated in this study.

Weight Ratio of ZIL:2-NP	LiTFSI Concentration (mol L^{-1})				
	DAEE-ZIL	**NMDE-ZIL**	**TBAE-ZIL**	**TEA-ZIL**	**2-NP**
1:1	1.00	1.00	1.00	1.00	1.00
	1.40	1.40	1.40	1.40	-
	1.80	1.80	1.80	1.80	-
	2.20	-	-	-	-
1:1.5	1.80	-	-	-	-
1.5:1	1.80	-	-	-	-

Figure 11 describes the temperature dependence ionic conductivity curves with varied LiTFSI contents in a 1:1 weight ratio of ZIL and 2-NP. As expected, the ionic conductivity increased with the increase of temperature, due to the decrease in viscosity. For each ZIL product, the ionic conductivities were measured at different LiTFSI concentrations to obtain optimum ionic conductivity. The results are summarized in Table 9. The formulations that displayed the most significant room temperature (298 K) ionic conductivity include: 1:1 TBAE-ZIL/2-NP (15.9 mS cm^{-1}) and 1.8 M in 1:1 DAEE-ZIL/2-NP (10.3 mS cm^{-1}). It is noteworthy that the former formulation possesses much superior ionic conductivity compared to the carbonate-based electrolytes (11 mS cm^{-1}) currently used in LIBs. High conductivity electrolytes are desirable for batteries with a high rate (>20 °C) charge/discharge features.

Table 9. The optimum ionic conductivity of 1:1 weight ratio of ZIL/2-NP mixtures containing optimum LiTFSI concentration.

	NMDE-ZIL	DAEE-ZIL	TBAE-ZIL	TEA-ZIL
The best ionic conductivity vs. LiTFSI concentration (mol L^{-1})	1.40	1.80	1.00	1.00
Ionic conductivity at 298 K (mS cm^{-1})	7.61	10.3	15.9	3.40
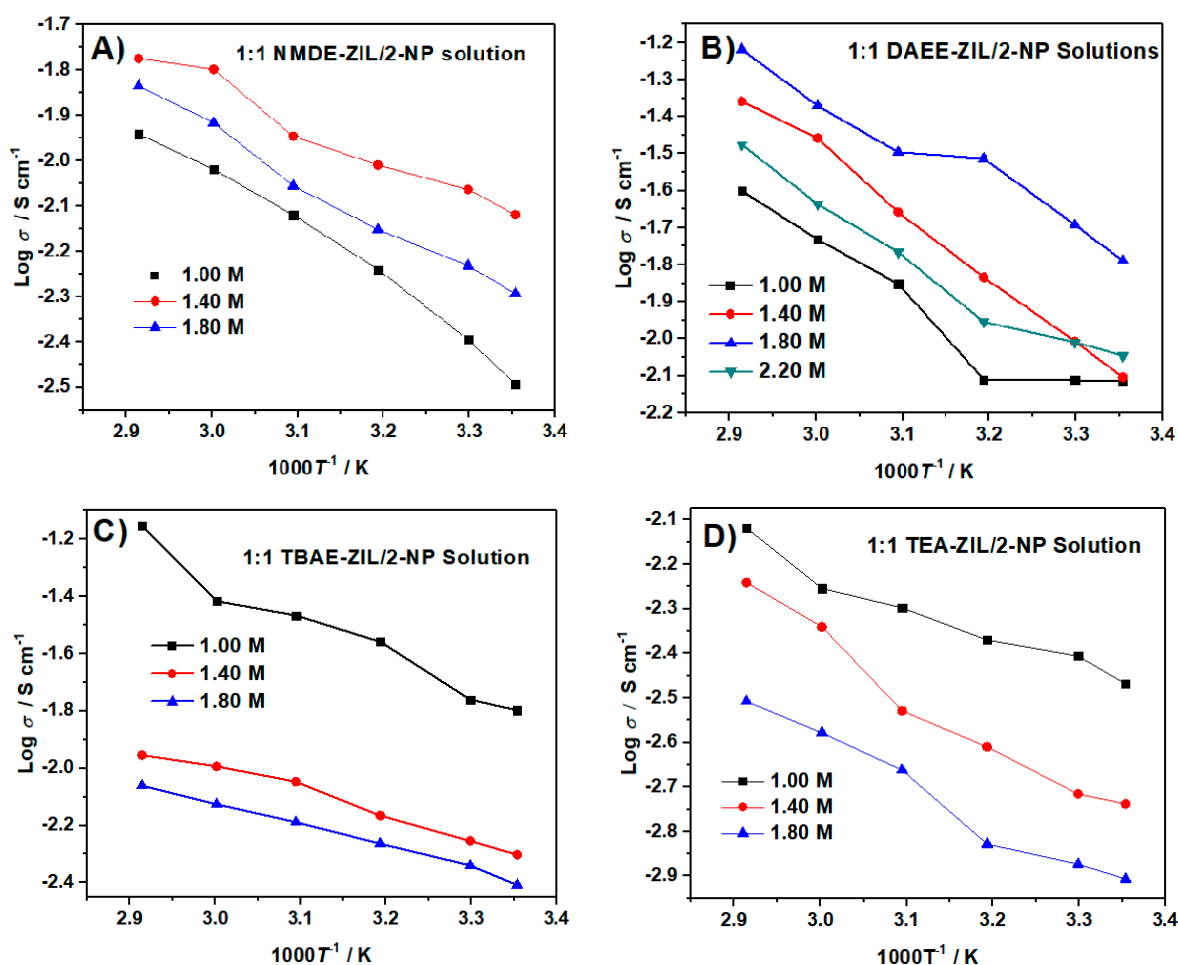
Figure 11. Temperature dependence of ionic conductivities of different LiTFSI concentrations of 1:1 weight ratio of (**A**) NMDE-ZIL, (**B**) DAEE-ZIL, (**C**) TBAE-ZIL, (**D**) TEA-ZIL and 2-NP solutions at the temperature range between 25 and 70 °C.

As depicted in Table 10, the ionic conductivity values of our ZIL-based electrolytes are also superior with respect to the values displayed by the recently published ZIL-based electrolytes. This display of high ionic conductivity of our ZIL-based electrolytes may be ascribed, due to the presence of numerous asymmetric coordination of Li^+ with the hemi-labile ligands (ether oxygen, amine nitrogen, and nitrile nitrogen) [89]. In general, chelates form more stable complexes than mono-dentate ligands. This is due to the fact that when one coordination site is detached, the entire ligand does not "fall off", and is, instead, still attached by the other coordination site. When both coordination sites are chemically equivalent, it is equally likely for each of the complexes to break off, which, in effect, stabilizes the chelate. In hemi-labile ligands, such as amino-ethers, the coordination sites are chemically nonequivalent—one site is weaker than the other, i.e., oxygen binds more strongly than nitrogen. These will form more stable complexes than two mono-dentate ligands but will allow much faster ligand exchange compared to chemically equivalent chelates. The increase in the rate of ligand exchange results from the substitution being directed by a 'trans effect'-like mechanism, which effectively makes it favorable for the oxygen of another ligand to be substituted in the position trans to the nitrogen. By directing ligand substitution in this way, the ionic conductivity will be improved as a result of allowing the lithium ions to be structurally transferred between two ligands to the same degree that they are vehicularly transferred by dragging with the ligands attached during conduction. The net effect is a system that kinetically favors the exchange of lithium ions between ligands rather than favor chelation with a single ligand.

Table 10. Comparison of ionic conductivity data: Present work vs. recently published work.

ZIL Electrolyte Compositions	Ionic Conductivity (mS cm^{-1})	References
[Py$_{1,1O1}$][FSA]/LiFSA/OE2pyps	4.2 (313 K)	[81]
G5/LiFSA/ImZ2	3.0 (298 K)	[90]
PEGDME/LiTFSA/CZ	0.24 (298 K)	[91]
DAEE-ZIL/2-NP/LiTFSI	10.3 (298 K)	Present work
TBAE/2-NP/LiTFSI	15.9 (298 K)	Present work

1M LiTFSI in pure 2-NP solution was also measured for comparison. We found that 2-NP electrolyte solution displayed ionic conductivity only at 4.09 mS cm^{-1} at room temperature, which was much lower than all of the ZIL-based electrolytes we investigated. This is because of a marked increase in the dielectric constant of the electrolytes, due to the addition of ZILs. We also noted limited dissolution of LiTFSI in 2-NP above 1 M concentration as we failed to prepare 1.4 M solution at room temperature. By contrast, we could easily prepare over 2 M LiTFSI solution with most 1:1 ZIL/2-NP mixture. This difference in solubility behavior is due to the increase of the dielectric constant of the solvent mixture in the presence of ZIL. An electrolyte with a high dielectric constant exhibits high ionic conductivity by promoting ionic dissociation of lithium salts [92]. Consequently, as we anticipated, the addition of ZIL materials to 2-NP remarkably increased both lithium salt solubility and ionic conductivity.

We have also studied the optimization of ionic conductivity of DAEE-ZIL in varied 2-NP content using 1.8 M LiTFSI concentration. The results are presented in Figure 12. A weight ratio of 1:1 was found to be the best combination for achieving high ionic conductivity. Increasing any component would deteriorate the performance of the electrolyte.
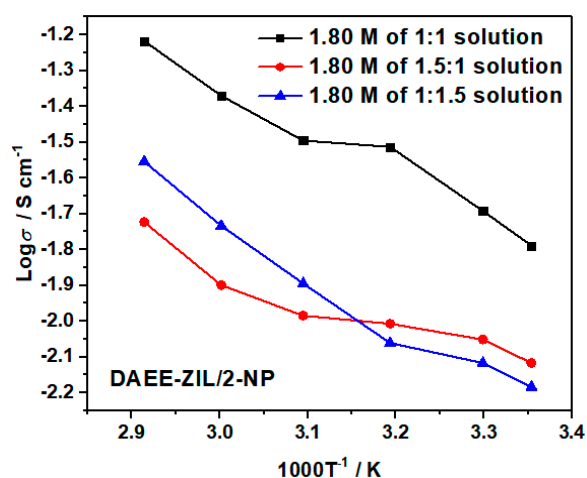
Figure 12. Ionic conductivities of 1.8 M LiTFSI in different weight ratios of DAEE-ZIL and 2-NP solutions.

3.5. Performance of IL Electrolytes-Based Supercapacitor Cells

Supercapacitors utilizing the electrical double layer capacitor (EDLC) principle offer the advantages of both conventional dielectric capacitors and rechargeable batteries, provide fast storing/releasing of high power, long cycling life, and high reversibility [93]. EDLCs store energy by electrostatic absorption of cations and anions at the interface between the electrode and electrolyte. This process involves no charge transfer between the electrode and electrolyte (i.e., non-faradic process). Due to this mechanism, the main advantages of EDLCs over batteries is their much higher charging/discharging rate (usually in seconds) and longer cycling life (usually >10,000 cycles) [94–97]. However, EDLCs are unpopular because of their energy density, which is 1–2 orders of magnitude lower than that of Li-ion batteries. As shown in the equation below, the energy density (*E*) of an EDLC device is proportional to its specific capacitance (**C**) and the square of its operating voltage (*V*).

$$E = \frac{1}{2}CV^2$$

Consequently, the energy density of an EDLC device can be increased by either achieving higher electrode capacitance and/or by expanding the operating voltage (OPV). Obviously, the adoption of electrolytes with a wide potential window is considered to be a more convenient strategy to increase the energy density voltage because of its square relationship with energy density.

Liquid electrolytes for EDLCs can be divided into three categories: Aqueous-based, IL-based and organic solvent-based [98–101]. Because of the redox potential window of H_2/O_2, the maximum OPV of the aqueous-based electrolyte is limited to ~1.0 V (for a strong acid/base electrolyte) or ~1.8 V (for neutral electrolyte). Despite all the advantages of aqueous electrolytes (such as high ionic conductivity), aqueous EDLCs cannot achieve high energy density because of lower OPV. IL-based electrolytes have been proven to provide maximum OPV as high as 3.5–3.7 V [100,102–104]. However, the high viscosity of ILs results in low electrolyte conductivity [18], leading to large internal resistance losses of the cells.

An electrolyte for EDLC influences not only the maximum OPV, but also specific capacitance. It is understood that the specific capacitance of an EDLC is also dictated by the availability of the pores on the electrode surface, which is closely related to the properties of the electrolyte, such as the sizes of cation and anion species and the ion-solvent interaction [105]. For the anionic species, BF_4^- is the best choice to increase the specific capacitance [105] because of its smaller size which not only means more anions can accumulate per unit surface area, but also provides accessibility to small pores on the electrode surface [106]. Furthermore, ILs based on BF_4^- usually provide higher electrochemical stability and ionic conductivity than other anions, such as $TFSI^-$ and PF_6^- [100,105]. Since neat ILs are not suitable for EDLC electrolytes we have prepared several electrolyte formulations based on 1-ethyl-3-methyl imidazolium tetrafluoroborate (EMIM-BF_4) and tetraethylammonium tetrafluoroborate (TEA-BF_4) in organic solvents, such as dimethoxyethane (DME) and ethylene carbonate (EC) (Table 11).

Table 11. The conductivity of electrolyte formulations designed in this study.

Electrolyte	Electrolyte Formulation [a]	χ (25 °C) (mS cm^{-1})	
		Our Measurement	**Literature Value**
#1	EMIM-BF_4/DME = 6/4	24.7	24.21
#2	EMIM-BF_4/DME = 4/6	Not miscible	
#3	EMIM-BF_4/EC/DME = 4/1/5	25.8	
#4	EMIM-BF_4/EC/DME = 4/3/3	26.8	
#5	1M TEA-BF_4 in DME	Not miscible	
#6	1M TEA-BF_4 in EC/DME = 1/4	Not miscible	
#7	1M TEA-BF_4 in EC/DME = 1/1	13.7	

[a] All solvents are in volume ratio.

The ionic conductivity measurement results met our expectations. Electrolytes #3 and #4 proved that a small proportion of EC could enhance the solubility of EMIM-BF_4; while a higher portion of EC displayed slightly better conductivity. Solution #7 proved that EC also increased the solubility of TEA-BF_4.

The maximum OPV of the EDLC coin cells was determined by the cyclic voltammetry (CV) experiment. We started from 0–2.5 V, and gradually increased the upper limit of OPV, until the redox peaks appeared at the high potential (the "sharp peak"), which indicates the oxidation reaction on the anode with the reduction in the electrolyte, and/or the reduction reaction on the cathode with the oxidation in the electrolyte. By this procedure, we could measure the approximate range of the maximum OPV (Figure 13). Sample #7 displayed the best ESW (3.25–3.50 V) among all formulations, i.e., high electrochemical stability of both the cation and anion.
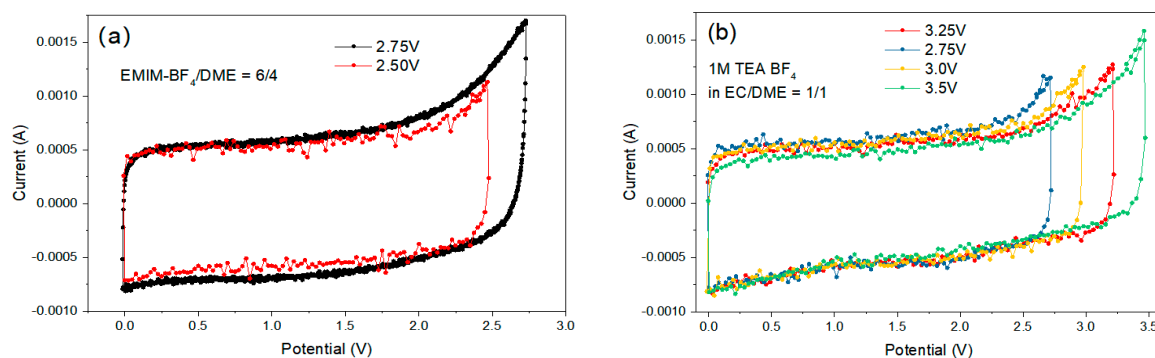
Figure 13. Cycling voltammetry curves of electrical double layer capacitors (EDLC) cells with formulations (**a**) #1, EMIM-BF4/DME = 6/4 *v/v*; (**b**) #7, 1M TEA-BF4 EC/DME = 1/1 *v/v*.

The cycling performances of the EDLC cells were examined by an MTI battery analyzer (BST8-WA). Coin cells with six different electrolyte formulations were run by charging-discharging cycles at different current densities: 0.5, 1.0, 2.0 and 4.0 A g^{-1}. The initial charging/discharging curves are presented in Figure 14.
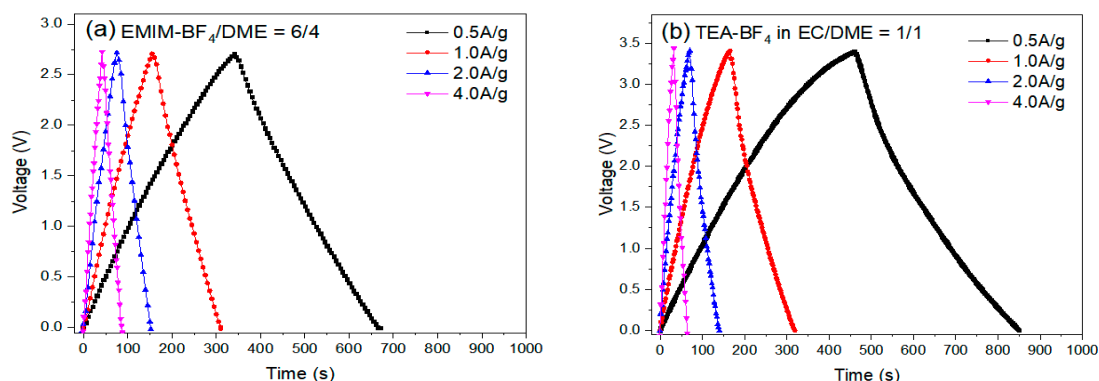
Figure 14. The initial charging-discharging curves at different current rates of EDLCs with electrolytes (**a**) #1, EMIM-BF4/DME = 6/4 *v/v*, (**b**) #7, 1M TEA-BF4 in EC/DME = 1/1 *v/v*.

Table 12 summarizes specific capacitance and energy density, which were calculated based on the initial (50th) cycle discharging time and OPV. The Coulombic efficiency (C_d/C_c) of the EDLC cells was calculated by discharging time/charging time of the displayed cycle at 1 A g^{-1}. Although electrolyte #1 showed the lowest internal resistance and a very good *C* value was observed (112.7 F g^{-1}), the lower OPV limits its energy density (29.6 Wh Kg^{-1}). By contrast, despite having a lower capacitance (87.9 F g^{-1}), electrolyte #7 displayed much higher energy density (37.4 Wh Kg^{-1}) because of higher OPV. The lower *C* is attributed to the larger size and sphere-like shape of TEA$^+$. The higher *C* of electrolyte #1 is likely due to the planar-shape of EMIM$^+$.

Table 12. Summary of the electrochemical properties of the EDLC cells with IL-based electrolytes.

	Electrolyte #1	Electrolyte #7
Electrolyte formulation	EMIM-BF$_4$/DME = 6/4 *v/v*	1M TEA-BF$_4$ in EC/DME = 1/1 *v/v*
Maximum OPV, (V)	2.5–2.75	3.25–3.5
Internal resistance, (Ohm)	~1.6	~3.7
Coulombic efficiency [a] C_d/C_c (%)	96.5	92.2
Initial specific discharge capacitance [a], C (F g^{-1})	112.7	87.9
Initial energy density [a], E (Wh kg^{-1})	29.6	37.4

[a] Data of the 50th cycle. Calculated at the current density of 1 A g^{-1}.

References

1. Schmuch, R.; Wagner, R.; Hörpel, G.; Placke, T.; Winter, M. Performance and cost of materials for lithium-based rechargeable automotive batteries. *Nat. Energy* **2018**, *3*, 267–278. [CrossRef]

2. Peters, J.F.; Baumann, M.; Zimmermann, B.; Braun, J.; Weil, M. The environmental impact of Li-Ion batteries and the role of key parameters—A review. *Renew. Sustain. Energy Rev.* **2017**, *67*, 491–506. [CrossRef]

3. Ordoñez, J.; Gago, E.J.; Girard, A. Processes and technologies for the recycling and recovery of spent lithium-ion batteries. *Renew. Sustain. Energy Rev.* **2016**, *60*, 195–205. [CrossRef]

4. Choi, J.W.; Aurbach, D. Promise and reality of post-lithium-ion batteries with high energy densities. *Nat. Rev. Mater.* **2016**, *1*, 16013. [CrossRef]

5. Appetecchi, G.B.; Montanino, M.; Passerini, S. *Ionic Liquids: Science and Applications*; Vissser, A.E., Bridges, N.J., Rogers, R.D., Eds.; ACS Symposium Series; Oxford University Press, Inc., American Chemical Society: Washington, DC, USA, 2013.

6. Goodenough, J.B.; Kim, Y. Challenges for rechargeable Li batteries. *Chem. Mater.* **2010**, *22*, 587–603. [CrossRef]

7. Balakrishnan, P.G.; Ramesh, R.; Prem Kumar, T. Safety mechanisms in lithium-ion batteries. *J. Power Sources* **2006**, *155*, 401–414. [CrossRef]

8. Wang, Y.; Li, B.; Ji, J.; Zhong, W.-H. Controlled Li$^+$ conduction pathway to achieve enhanced ionic conductivity in polymer electrolytes. *J. Power Sources* **2014**, *247*, 452–459. [CrossRef]

9. Wang, Y.; Zhong, W.-H. Development of Electrolytes towards Achieving Safe and High-Performance Energy-Storage Devices: A Review. *ChemElectroChem* **2015**, *2*, 22–36. [CrossRef]

10. Wang, L.; Li, X.; Yang, W. Enhancement of electrochemical properties of hot-pressed poly(ethylene oxide)-based nanocomposite polymer electrolyte films for all-solid-state lithium polymer batteries. *Electrochim. Acta* **2010**, *55*, 1895–1899. [CrossRef]

11. Prasanth, R.; Shubha, N.; Hng, H.H.; Srinivasan, M. Effect of poly(ethylene oxide) on ionic conductivity and electrochemical properties of poly(vinylidenefluoride) based polymer gel electrolytes prepared by electrospinning for lithium ion batteries. *J. Power Sources* **2014**, *245*, 283–291. [CrossRef]

12. Shubha, N.; Prasanth, R.; Hoon, H.H.; Srinivasan, M. Plastic crystalline-semi crystalline polymer composite electrolyte based on non-woven poly(vinylidenefluoride-co-hexafluoropropylene) porous membranes for lithium ion batteries. *Electrochim. Acta* **2014**, *125*, 362–370. [CrossRef]

13. Lei, Z.; Chen, B.; Koo, Y.-M.; MacFarlane, D.R. Introduction: Ionic Liquids. *Chem. Rev.* **2017**, *117*, 6633–6635. [CrossRef] [PubMed]

14. Yim, T.; Kwon, M.-S.; Mun, J.; Lee, K.T. Room Temperature Ionic Liquid-based Electrolytes as an Alternative to Carbonate-based Electrolytes. *Isr. J. Chem.* **2015**, *55*, 586–598. [CrossRef]

15. Zhang, S.; Zhang, Q.; Zhang, Y.; Chen, Z.; Watanabe, M.; Deng, Y. Beyond solvents and electrolytes: Ionic liquids-based advanced functional materials. *Prog. Mater. Sci.* **2016**, *77*, 80–124. [CrossRef]

16. Jin, Y.; Fang, S.; Chai, M.; Yang, L.; Tachibana, K.; Hirano, S. Properties and application of ether-functionalized trialkylimidazolium ionic liquid electrolytes for lithium battery. *J. Power Sources* **2013**, *226*, 210–218. [CrossRef]

17. Sun, X.G.; Liao, C.; Shao, N.; Bell, J.R.; Guo, B.; Luo, H.; Jiang, D.E.; Dai, S. Bicyclic imidazolium ionic liquids as potential electrolytes for rechargeable lithium ion batteries. *J. Power Sources* **2013**, *237*, 5–12. [CrossRef]

18. Levchuk, I.; Rueda Márquez, J.J.; Sillanpää, M. Removal of natural organic matter (NOM) from water by ion exchange—A review. *Chemosphere* **2018**, *192*, 90–104. [CrossRef]

19. Zhang, J.-N.; Li, Q.; Wang, Y.; Zheng, J.; Yu, X.; Li, H. Dynamic evolution of cathode electrolyte interphase (CEI) on high voltage LiCoO$_2$ cathode and its interaction with Li anode. *Energy Storage Mater.* **2018**, *14*, 1–7. [CrossRef]

20. Brandt, A.; Pohlmann, S.; Varzi, A.; Balducci, A.; Passerini, S. Ionic liquids in supercapacitors. *MRS Bull.* **2013**, *38*, 554–559. [CrossRef]

21. Varzi, A.; Schütter, C.; Krummacher, J.; Raccichini, R.; Wolff, C.; Kim, G.-T.; Rosler, S.; Blumenroder, B.; Schubert, T.; Passerini, S.; et al. A 4 Farad high energy electrochemical double layer capacitor prototype operating at 3.2 V (IES prototype). *J. Power Sources* **2016**, *326*, 162–169. [CrossRef]

22. Yuyama, K.; Masuda, G.; Yoshida, H.; Sato, T. Ionic liquids containing the tetrafluoroborate anion have the best performance and stability for electric double layer capacitor applications. *J. Power Sources* **2006**, *162*, 1401–1408. [CrossRef]

23. Sato, T.; Masuda, G.; Takagi, K. Electrochemical properties of novel ionic liquids for electric double layer capacitor applications. *Electrochim. Acta* **2004**, *49*, 3603–3611. [CrossRef]

24. Kim, Y.-J.; Matsuzawa, Y.; Ozaki, S.; Park, K.C.; Kim, C.; Endo, M.; Yoshida, H.; Masuda, G.; Sato, T.; Dresselhaus, M.S. High Energy-Density Capacitor Based on Ammonium Salt Type Ionic Liquids and Their Mixing Effect by Propylene Carbonate. *J. Electrochem. Soc.* **2005**, *152*, A710. [CrossRef]

25. Sato, T.; Marukane, S.; Morinaga, T.; Kamijo, T.; Arafune, H.; Tsujii, Y. High voltage electric double layer capacitor using a novel solid-state polymer electrolyte. *J. Power Sources* **2015**, *295*, 108–116. [CrossRef]

26. Maruyama, Y.; Marukane, S.; Morinaga, T.; Honma, S.; Kamijo, T.; Shomura, R.; Sato, T. New design of polyvalent ammonium salts for a high-capacity electric double layer capacitor. *J. Power Sources* **2019**, *412*, 18–28. [CrossRef]

27. Plechkova, N.V.; Seddon, K.R. Applications of ionic liquids in the chemical industry. *Chem. Soc. Rev.* **2008**, *37*, 123–150. [CrossRef] [PubMed]

28. Kang, X.; Sun, X.; Han, B. Synthesis of Functional Nanomaterials in Ionic Liquids. *Adv. Mater.* **2015**, *28*, 1011–1030. [CrossRef]

29. Raccichini, R.; Varzi, A.; Chakravadhanula, V.S.K.; Kübel, C.; Balducci, A.; Passerini, S. Enhanced low-temperature lithium storage performance of multilayer graphene made through an improved ionic liquid-assisted synthesis. *J. Power Sources* **2015**, *281*, 318–325. [CrossRef]

30. Yue, Z.; Mei, X.; Dunya, H.; Ma, Q.; McGarry, C.; Mandal, B.K. Synthesis and physical properties of new fluoroether sulfones. *J. Fluor. Chem.* **2018**, *216*, 118–123. [CrossRef]

31. McCrary, P.D.; Chatel, G.; Alaniz, S.A.; Cojocaru, O.A.; Beasley, P.A.; Flores, L.A.; Kelley, S.P.; Barber, P.S.; Rogers, R.D. Evaluating Ionic Liquids as Hypergolic Fuels: Exploring Reactivity from Molecular Structure. *Energy Fuels* **2014**, *28*, 3460–3473. [CrossRef]

32. Takao, K.; Ikeda, Y. Alternative Route to Metal Halide Free Ionic Liquids. *Chem. Lett.* **2008**, *37*, 682–683. [CrossRef]

33. Mei, X.; Yue, Z.; Tufts, J.; Dunya, H.; Mandal, B.K. Synthesis of new fluorine-containing room temperature ionic liquids and their physical and electrochemical properties. *J. Fluor. Chem.* **2018**, *212*, 26–37. [CrossRef]

34. Choi, J.A.; Shim, E.G.; Scrosati, B.; Kim, D.W. Mixed electrolytes of organic solvents and ionic liquid for rechargeable lithium-ion batteries. *Bull. Korean Chem. Soc.* **2010**, *31*, 190–3194. [CrossRef]

35. Lalia, B.S.; Yoshimoto, N.; Egashira, M.; Morita, M. A mixture of triethylphosphate and ethylene carbonate as a safe additive for ionic liquid-based electrolytes of lithium ion batteries. *J. Power Sources* **2010**, *195*, 7426–7431. [CrossRef]

36. Arbizzani, C.; Gabrielli, G.; Mastragostino, M. Thermal stability and flammability of electrolytes for lithium-ion batteries. *J. Power Sources* **2011**, *196*, 4801–4805. [CrossRef]

37. Nakagawa, H.; Fujino, Y.; Kozono, S.; Katayama, Y.; Nukuda, T.; Sakaebe, H.; Matsumoto, H.; Tatsumi, K. Application of nonflammable electrolyte with room temperature ionic liquids (RTILs) for lithium-ion cells. *J. Power Sources* **2007**, *174*, 1021–1026. [CrossRef]

38. Suo, L.; Hu, Y.-S.; Li, H.; Armand, M.; Chen, L. A new class of Solvent-in-Salt electrolyte for high-energy rechargeable metallic lithium batteries. *Nat. Commun.* **2013**, *4*, 1481. [CrossRef]

39. Park, M.; Zhang, X.; Chung, M.; Less, G.B.; Sastry, A.M. A review of conduction phenomena in Li-ion batteries. *J. Power Sources* **2010**, *195*, 7904–7929. [CrossRef]

40. Makino, T.; Kanakubo, M.; Umecky, T.; Suzuki, A.; Nishida, T.; Takano, J. Electrical Conductivities, Viscosities, and Densities of *N*-Methoxymethyl- and *N*-Butyl-*N*-methylpyrrolidinium Ionic Liquids with the Bis(fluorosulfonyl)amide Anion. *J. Chem. Eng. Data* **2012**, *57*, 751–755. [CrossRef]

41. Zhou, Z.-B.; Matsumoto, H.; Tatsumi, K. Cyclic Quaternary Ammonium Ionic Liquids with Perfluoroalkyltrifluoroborates: Synthesis, Characterization, and Properties. *Chem. A Eur. J.* **2006**, *12*, 2196–2212. [CrossRef]

42. Orita, A.; Kamijima, K.; Yoshida, M. Allyl-functionalized ionic liquids as electrolytes for electric double-layer capacitors. *J. Power Sources* **2010**, *195*, 7471–7479. [CrossRef]

43. Wu, T.-Y.; Su, S.-G.; Wang, H.P.; Lin, Y.-C.; Gung, S.-T.; Lin, M.-W.; Sun, I.-W. Electrochemical studies and self diffusion coefficients in cyclic ammonium based ionic liquids with allyl substituents. *Electrochim. Acta* **2011**, *56*, 3209–3218. [CrossRef]

44. Fu, S.; Gong, S.; Liu, C.; Zheng, L.; Feng, W.; Nie, J.; Zhou, Z. Ionic liquids based on bis(2,2,2-trifluoroethoxysulfonyl)imide with various oniums. *Electrochim. Acta* **2013**, *94*, 229–237. [CrossRef]

45. Carvalho, P.J.; Regueira, T.; Santos, L.M.N.B.F.; Fernandez, J.; Coutinho, J.A.P. Effect of Water on the Viscosities and Densities of 1-Butyl-3-methylimidazolium Dicyanamide and 1-Butyl-3-methylimidazolium Tricyanomethane at Atmospheric Pressure. *J. Chem. Eng. Data* **2010**, *55*, 645–652. [CrossRef]

46. Sánchez, L.G.; Espel, J.R.; Onink, F.; Meindersma, G.W.; de Haan, A.B. Density, Viscosity, and Surface Tension of Synthesis Grade Imidazolium, Pyridinium, and Pyrrolidinium Based Room Temperature Ionic Liquids. *J. Chem. Eng. Data* **2009**, *54*, 2803–2812. [CrossRef]

47. Zech, O.; Stoppa, A.; Buchner, R.; Kunz, W. The Conductivity of Imidazolium-Based Ionic Liquids from (248 to 468) KB Variation of the Anion. *J. Chem. Eng. Data* **2010**, *55*, 1774–1778. [CrossRef]

48. Bulut, S.; Eiden, P.; Beichel, W.; Slattery, J.M.; Beyersdorff, T.F.; Schubert, T.J.S.; Krossing, I. Temperature dependence of the viscosity and conductivity of mildly functionalized and non-functionalized [Tf2N]-ionic liquids. *ChemPhysChem* **2011**, *12*, 2296–2310. [CrossRef] [PubMed]

49. Bini, R.; Malvaldi, M.; Pitner, W.R.; Chiappe, C. QSPR correlation for conductivities and viscosities of low-temperature melting ionic liquids. *J. Phys. Org. Chem.* **2008**, *21*, 622–629. [CrossRef]

50. Chen, Z.J.; Xue, T.; Lee, J.M. What causes the low viscosity of ether-functionalized ionic liquids? Its dependence on the increase of free volume. *RSC Adv.* **2012**, *2*, 10564–10574. [CrossRef]

51. Nakamura, K.; Shikata, T. Systematic Dielectric and NMR Study of the Ionic Liquid 1-Alkyl-3-Methyl Imidazolium. *ChemPhysChem* **2010**, *11*, 285–294. [CrossRef]

52. Bedrov, D.; Borodin, O.; Li, Z.; Smith, G.D. Influence of Polarization on Structural, Thermodynamic, and Dynamic Properties of Ionic Liquids Obtained from Molecular Dynamics Simulations. *J. Phys. Chem. B* **2010**, *114*, 4984–4997. [CrossRef] [PubMed]

53. Stoppa, A.; Hunger, J.; Buchner, R. Conductivities of Binary Mixtures of Ionic Liquids with Polar Solvents. *J. Chem. Eng. Data* **2009**, *54*, 472–479. [CrossRef]

54. Mei, X.; Yue, Z.; Ma, Q.; Dunya, H.; Mandal, B.K. Synthesis and electrochemical properties of new dicationic ionic liquids. *J. Mol. Liq.* **2018**, *272*, 1001–1018. [CrossRef]

55. Coadou, E.; Goodrich, P.; Neale, A.R.; Timperman, L.; Hardacre, C.; Jacquemin, J.; Anouti, M. Synthesis and Thermophysical Properties of Ether-Functionalized Sulfonium Ionic Liquids as Potential Electrolytes for Electrochemical Applications. *ChemPhysChem* **2016**, *17*, 3992–4002. [CrossRef]

56. Rennie, A.J.R.; Martins, V.L.; Torresi, R.M.; Hall, P.J. Ionic Liquids Containing Sulfonium Cations as Electrolytes for Electrochemical Double Layer Capacitors. *J. Phys. Chem. C* **2015**, *119*, 23865–23874. [CrossRef]

57. Gerhard, D.; Alpaslan, S.C.; Gores, H.J.; Uerdingen, M.; Wasserscheid, P. Trialkylsulfonium dicyanamides—A new family of ionic liquids with very low viscosities. *Chem. Commun.* **2005**, *40*, 5080–5082. [CrossRef]

58. Gerhard, D.; Alpaslan, S.C.; Gores, H.J.; Uerdingen, M.; Wasserscheid, P. Imidazolium-Based Ionic Liquids Formed with Dicyanamide Anion: Influence of Cationic Structure on Ionic Conductivity. *J. Phys. Chem. B* **2007**, *111*, 12204–12210. [CrossRef]

59. Zhang, Q.; Liu, S.; Li, Z.; Li, J.; Chen, Z.; Wang, R.; Lu, L.; Deng, Y. Novel Cyclic Sulfonium-Based Ionic Liquids: Synthesis, Characterization, and Physicochemical Properties. *Chem. A Eur. J.* **2009**, *15*, 765–778. [CrossRef]

60. Zhao, D.; Fei, Z.; Ang, W.; Dyson, P. Sulfonium-based Ionic Liquids Incorporating the Allyl Functionality. *Int. J. Mol. Sci.* **2007**, *8*, 304–315. [CrossRef]

61. MacFarlane, D.R.; Golding, J.; Forsyth, S.; Forsyth, M.; Deacon, G.B. Low viscosity ionic liquids based on organic salts of the dicyanamide anion. *Chem. Commun.* **2001**, *16*, 1430–1431. [CrossRef]

62. Marcilla, A.; Ruiz, F.; García, A.N. Liquid-liquid-solid equilibria of the quaternary system water-ethanol-acetone-sodium chloride at 25 °C. *Fluid Phase Equilib.* **1995**, *112*, 273–289. [CrossRef]

63. Xue, H.; Shreeve, J.M. Ionic liquids with fluorine-containing cations. *Eur. J. Inorg. Chem.* **2005**, *13*, 2573–2580. [CrossRef]

64. Pereiro, A.B.; Araújo, J.M.M.; Martinho, S.; Alves, F.; Nunes, S.; Matias, A.; Duarte, C.M.M.; Rebelo, L.P.N.; Marrucho, I.M. Fluorinated ionic liquids: Properties and applications. *ACS Sustain. Chem. Eng.* **2013**, *1*, 427–439. [CrossRef]

65. Davis, J.H.; Forrester, K.J.; Merrigan, T. Novel organic ionic liquids (OILS) incorporating cations derived from the antifungal drug miconazole. *Tetrahedron Lett.* **1998**, *39*, 8955–8958. [CrossRef]

66. Vanhoutte, G.; Hojniak, S.D.; Bardé, F.; Binnemans, K.; Fransaer, J. Fluorine-functionalized ionic liquids with high oxygen solubility. *RSC Adv.* **2018**, *8*, 4525–4530. [CrossRef]

67. Bonhôte, P.; Dias, A.-P.; Papageorgiou, N.; Kalyanasundaram, K.; Grätzel, M. Hydrophobic Highly Conductive Ambient-Temperature Molten Salts. *Inorg. Chem.* **1996**, *35*, 1168–1178. [CrossRef] [PubMed]

68. Merrigan, T.L.; Bates, E.D.; Dorman, S.C.; Davis, J.H., Jr. New fluorous ionic liquids function as surfactants in conventional room-temperature ionic liquids. *Chem. Commun.* **2000**, 2051–2052. [CrossRef]

69. Tindale, J.J.; Mouland, K.L.; Ragogna, P.J. Thiol appended, fluorinated phosphonium ionic liquids as covalent superhydrophobic coatings. *J. Mol. Liq.* **2010**, *152*, 14–18. [CrossRef]

70. McMillan, R.; Slegr, H.; Shu, Z.; Wang, W. Fluoroethylene carbonate electrolyte and its use in lithium ion batteries with graphite anodes. *J. Power Sources* **1999**, *81–82*, 20–26. [CrossRef]

71. Xu, K.; Zhang, S.; Allen, J.L.; Jow, T.R. Nonflammable Electrolytes for Li-Ion Batteries Based on a Fluorinated Phosphate. *J. Electrochem. Soc.* **2002**, *149*, A1079. [CrossRef]

72. Banks, R.E.; Smart, B.E.; Tatlow, J.C. (Eds.) *Organofluorine Chemistry: Principles and Commercial Applications*, 1st ed.; Springer: Boston, MA, USA, 1994.

73. Yoon, H.; Lane, G.H.; Shekibi, Y.; Howlett, P.C.; Forsyth, M.; Best, A.S.; MacFarlane, D.R. Lithium electrochemistry and cycling behaviour of ionic liquids using cyano based anions. *Energy Environ. Sci.* **2013**, *6*, 979. [CrossRef]

74. Lee, J.S.; Quan, N.D.; Hwang, J.M.; Bae, J.Y.; Kim, H.; Cho, B.W.; Kim, H.S.; Lee, H. Ionic liquids containing an ester group as potential electrolytes. *Electrochem. Commun.* **2006**, *8*, 460–464. [CrossRef]

75. Chakrabarti, A.; Filler, R.; Mandal, B.K. Synthesis and properties of a new class of fluorine-containing dilithium salts for lithium-ion batteries. *Solid State Ion.* **2010**, *180*, 1640–1645. [CrossRef]

76. Zhang, Z.; Zhou, H.; Yang, L.; Tachibana, K.; Kamijima, K.; Xu, J. Asymmetrical dicationic ionic liquids based on both imidazolium and aliphatic ammonium as potential electrolyte additives applied to lithium secondary batteries. *Electrochim. Acta* **2008**, *53*, 4833–4838. [CrossRef]

77. Tadesse, H.; Blake, A.J.; Champness, N.R.; Warren, J.E.; Rizkallah, P.J.; Licence, P. Supramolecular architectures of symmetrical dicationic ionic liquid based systems. *CrystEngComm* **2012**, *14*, 4886. [CrossRef]

78. Anderson, J.L.; Ding, R.; Ellern, A.; Armstrong, D.W. Structure and Properties of High Stability Geminal Dicationic Ionic Liquids. *J. Am. Chem. Soc.* **2005**, *127*, 593–604. [CrossRef] [PubMed]

79. Kubisa, P.; Biedroń, T. Poly(oxyethylene)s terminated at both ends with phosphonium ion end groups, 2. Properties. *Macromol. Chem. Phys.* **1996**, *197*, 31–40. [CrossRef]

80. Suematsu, M.; Yoshizawa-Fujita, M.; Tamura, T.; Takeoka, Y.; Rikukawa, M. Dependence of transport properties of concentrated lithium salt solutions on temperature and composition in an imidazolium-based liquid zwitterion containing an oligo(ethylene oxide) unit. *Int. J. Electrochem. Sci.* **2015**, *10*, 248–258.

81. Horiuchi, S.; Zhu, H.; Forsyth, M.; Takeoka, Y.; Rikukawa, M.; Yoshizawa-Fujita, M. Synthesis and evaluation of a novel pyrrolidinium-based zwitterionic additive with an ether side chain for ionic liquid electrolytes in high-voltage lithium-ion batteries. *Electrochim. Acta* **2017**, *241*, 272–280. [CrossRef]

82. Yoshizawa-Fujita, M.; Tamura, T.; Takeoka, Y.; Rikukawa, M. Low-melting zwitterion: Effect of oxyethylene units on thermal properties and conductivity. *Chem. Commun.* **2011**, *47*, 2345–2347. [CrossRef]

83. Ma, Q.; Mandal, B.K. Highly Conductive Electrolytes Derived from Nitrile Solvents. *J. Electrochem. Soc.* **2015**, *162*, A1276–A1281. [CrossRef]

84. Lane, G.H.; Best, A.S.; MacFarlane, D.R.; Forsyth, M.; Bayley, P.M.; Hollenkamp, A.F. The electrochemistry of lithium in ionic liquid/organic diluent mixtures. *Electrochim. Acta* **2010**, *55*, 8947–8952. [CrossRef]

85. Hofmann, A.; Schulz, M.; Hanemann, T. Effect of conducting salts in ionic liquid based electrolytes: Viscosity, conductivity, and li-ion cell studies. *Int. J. Electrochem. Sci.* **2013**, *8*, 10170–10189.

86. Wu, F.; Zhu, Q.; Chen, R.; Chen, N.; Chen, Y.; Li, L. Ring-chain synergy in ionic liquid electrolytes for lithium batteries. *Chem. Sci.* **2015**, *6*, 7274–7283. [CrossRef] [PubMed]

87. Le, L.T.M.; Vo, T.D.; Ngo, K.H.P.; Okada, S.; Alloin, F.; Garg, A.; Le, P.M.L. Mixing ionic liquids and ethylene carbonate as safe electrolytes for lithium-ion batteries. *J. Mol. Liq.* **2018**, *271*, 769–777. [CrossRef]

88. Väli, R.; Jänes, A.; Lust, E. Vinylene Carbonate as Co-Solvent for Low-Temperature Mixed Electrolyte Based Supercapacitors. *J. Electrochem. Soc.* **2016**, *163*, A851–A857. [CrossRef]

89. Ramírez, A.; Lobkovsky, E.; Collum, D.B. Hemilabile Ligands in Organolithium Chemistry: Substituent Effects on Lithium Ion Chelation. *J. Am. Chem. Soc.* **2003**, *125*, 15376–15387. [CrossRef] [PubMed]

90. Suematsu, M.; Yoshizawa-Fujita, M.; Zhu, H.; Forsyth, M.; Takeoka, Y.; Rikukawa, M. Effect of zwitterions on electrochemical properties of oligoether-based electrolytes. *Electrochim. Acta* **2015**, *175*, 209–213. [CrossRef]

91. Yamaguchi, S.; Yoshizawa-Fujita, M.; Zhu, H.; Forsyth, M.; Takeoka, Y.; Rikukawa, M. Improvement of charge/discharge properties of oligoether electrolytes by zwitterions with an attached cyano group for use in lithium-ion secondary batteries. *Electrochim. Acta* **2015**, *186*, 471–477. [CrossRef]

92. Lu, W.; Xie, K.; Chen, Z.; Xiong, S.; Pan, Y.; Zheng, C. A new co-solvent for wide temperature lithium ion battery electrolytes: 2,2,2-Trifluoroethyl n-caproate. *J. Power Sources* **2015**, *274*, 676–684. [CrossRef]

93. Suda, Y.; Mizutani, A.; Harigai, T.; Takikawa, H.; Ue, H.; Umeda, Y. Influences of internal resistance and specific surface area of electrode materials on characteristics of electric double layer capacitors. In *AIP Conference Proceedings*; AIP Publishing: Melville, NY, USA, 2017; p. 020022.

94. Simon, P.; Gogotsi, Y.; Dunn, B. Where Do Batteries End and Supercapacitors Begin? *Science* **2014**, *343*, 1210–1211. [CrossRef] [PubMed]

95. Choi, N.-S.; Chen, Z.; Freunberger, S.A.; Ji, X.; Sun, Y.-K.; Amine, K.; Yushin, G.; Nazar, L.F.; Cho, J.; Bruce, P.G. Challenges Facing Lithium Batteries and Electrical Double-Layer Capacitors. *Angew. Chem. Int. Ed.* **2012**, *51*, 9994–10024. [CrossRef] [PubMed]

96. Gu, W.; Yushin, G. Review of nanostructured carbon materials for electrochemical capacitor applications: Advantages and limitations of activated carbon, carbide-derived carbon, zeolite-templated carbon, carbon aerogels, carbon nanotubes, onion-like carbon, and graphene. *Wiley Interdiscip. Rev. Energy Environ.* **2014**, *3*, 424–473. [CrossRef]

97. González, A.; Goikolea, E.; Barrena, J.A.; Mysyk, R. Review on supercapacitors: Technologies and materials. *Renew. Sustain. Energy Rev.* **2016**, *58*, 1189–1206. [CrossRef]

98. Zhong, C.; Deng, Y.; Hu, W.; Qiao, J.; Zhang, L.; Zhang, J. A review of electrolyte materials and compositions for electrochemical supercapacitors. *Chem. Soc. Rev.* **2015**, *44*, 7484–7539. [CrossRef] [PubMed]

99. Wu, Z.; Li, L.; Yan, J.; Zhang, X. Materials Design and System Construction for Conventional and New-Concept Supercapacitors. *Adv. Sci.* **2017**, *4*, 1600382. [CrossRef] [PubMed]

100. Lewandowski, A.; Olejniczak, A.; Galinski, M.; Stepniak, I. Performance of carbon–carbon supercapacitors based on organic, aqueous and ionic liquid electrolytes. *J. Power Sources* **2010**, *195*, 5814–5819. [CrossRef]

101. Béguin, F.; Presser, V.; Balducci, A.; Frackowiak, E. Carbons and Electrolytes for Advanced Supercapacitors. *Adv. Mater.* **2014**, *26*, 2219–2251. [CrossRef] [PubMed]

102. Tsai, W.-Y.; Lin, R.; Murali, S.; Zhang, L.L.; McDonough, J.K.; Ruoff, R.S.; Taberna, P.-L.; Gogotsi, Y.; Simon, P. Outstanding performance of activated graphene based supercapacitors in ionic liquid electrolyte from −50 to 80 °C. *Nano Energy* **2013**, *2*, 403–411. [CrossRef]

103. Van Aken, K.L.; Beidaghi, M.; Gogotsi, Y. Formulation of ionic-liquid electrolyte to expand the voltage window of supercapacitors. *Angew. Chem. Int. Ed.* **2015**, *54*, 4806–4809. [CrossRef]

104. Biso, M.; Mastragostino, M.; Montanino, M.; Passerini, S.; Soavi, F. Electropolymerization of poly(3-methylthiophene) in pyrrolidinium-based ionic liquids for hybrid supercapacitors. *Electrochim. Acta* **2008**, *53*, 7967–7971. [CrossRef]

105. Mousavi, M.P.S.; Wilson, B.E.; Kashefolgheta, S.; Anderson, E.L.; He, S.; Bühlmann, P.; Stein, A. Ionic Liquids as Electrolytes for Electrochemical Double-Layer Capacitors: Structures that Optimize Specific Energy. *ACS Appl. Mater. Interfaces* **2016**, *8*, 3396–3406. [CrossRef] [PubMed]

106. Largeot, C.; Portet, C.; Chmiola, J.; Taberna, P.-L.; Gogotsi, Y.; Simon, P. Relation between the Ion Size and Pore Size for an Electric Double-Layer Capacitor. *J. Am. Chem. Soc.* **2008**, *130*, 2730–2731. [CrossRef] [PubMed]